

Verification of calculation code **THERM** in accordance with **BS EN ISO 10077-2**



Lead author:

Sathish K.Nammi (sathish.nammi@anglia.ac.uk)

Co-authors:

Hassan Shirvani (Hassan.Shirvani@anglia.ac.uk)

Ayoub Shirvani (Ayoub.Shirvani@anglia.ac.uk)

Gerard Edwards (G.Edwards@bolton.ac.uk)

Justin P.M.Whitty (jwhitty@uclan.ac.uk)

Any enquiries about or comments on this publication should be directed to:

Engineering Analysis, Simulation and Tribology (EAST) Research Group

Anglia Ruskin University,

Bishop Hall Lane,

Chelmsford,

UK - CM1 1SQ

Tel: 08451963900

ISBN: 978-0-9565608-8-9

Date: August 2014

Executive Summary:

Calculation codes are useful in predicting the heat transfer features in the fenestration industry. THERM is a finite element analysis based code, which can be used to compute thermal transmittance of windows, doors and shutters. It is important to verify results of THERM as per BS EN ISO 10077-2 to meet the compliance requirements. In this report, two-dimensional thermal conductance parameters were computed. Three versions of THERM, 5.2, 6.3 and 7.1, were used at two successive finite element mesh densities to assess their comparability. The results were all compliant with the aforementioned British Standard.

Disclaimer:

This document was prepared for research purposes. The authors make no warranty for the accuracy or validity of the information contained in this report. The authors or any agency cannot be held responsible for any errors or inaccuracies in this report. This is an independent report and it does not necessarily constitute or imply its endorsement by THERM of Lawrence Berkeley National Laboratory or International Organization for Standard.

Acknowledgements:

The authors would like to thank Low Carbon KEEP (Knowledge East of England Partnership), European Regional Development Fund (ERDF) and East of England Development Agency for funding this research. Acknowledgements also go to our project partners Mr Jeremy Dunn and Mr James Botwright of Glazing Vision Ltd. Special thanks to Mr Jean-Luc Mauricette for valuable suggestions.

Copyright:

The content of this work is protected by copyright, with all rights reserved. This technical report is released under a Creative Commons License.

Contents:

Executive Summary:	iii
Disclaimer:	iii
Acknowledgements:	iv
Copyright:	iv
List of Figures	viii
List of Tables	x
Terms, definitions and symbols:	xi
1. Introduction	1
1.1 Structure of this report	2
1.2 Finite element analysis (FEA)	3
1.3 General methodology	5
1.3.1 Pre-processing	5
1.3.2 Solving	5
1.3.3 Post-processing	6
1.4 Calculation programme THERM	6
2. Background	9
2.1 Modes of heat transfer	9
2.1.1 Conduction	9
2.1.2 Convection	11

2.1.3	Radiation -----	12
2.2	Frame cavities -----	13
2.2.1	Convective heat transfer coefficient -----	16
2.2.2	Radiative heat transfer coefficient -----	18
2.3	One-dimensional steady-state heat transfer -----	21
2.3.1	Plane slab -----	22
2.3.2	Composite panel -----	27
2.4	Surface resistances -----	32
2.5	Calculation of thermal transmittance -----	33
2.5.1	Windows and doors -----	34
2.5.2	Shutters -----	37
3.	Centre-pane thermal transmittance values -----	38
3.1	Insulation panel -----	38
3.2	Two-pane glazing unit -----	40
4.	Computer simulations -----	42
4.1	Example-1 -----	46
4.2	Example-2 -----	50
4.3	Example-3 -----	53
4.4	Example-4 -----	56
4.5	Example-5 -----	60
4.6	Example-6 -----	63
4.7	Example-7 -----	67
4.8	Example-8 -----	71

4.9	Example-9	75
4.10	Example-10	78
5.	Conclusions	82
	References	85

List of Figures

Figure 2.2.a: Illustration of a rectangular cavity -----	17
Figure 2.2.b: Transformation of a non-rectangular cavity -----	21
Figure 2.3.a: Illustration of a plane slab -----	22
Figure 2.3.b: Illustration of a three layered composite panel -----	28
Figure 2.5.a: Schematic of frame section with an insulation panel -----	36
Figure 2.5.b: Schematic of frame section with IGU -----	37
Figure 3.1.a: Illustration of boundary conditions on the insulation panel-----	39
Figure 3.2.a: THERM model of IGU -----	41
Figure 4.1.a: Illustration of example-1 -----	48
Figure 4.1.b: Air cavities of example-1-----	48
Figure 4.1.c: Illustration of boundaries of example-1-----	49
Figure 4.1.d: 2D thermal conductance and temperature distribution map of example-1-----	49
Figure 4.2.a: Illustration of example-2 -----	51
Figure 4.2.b: Unventilated air cavities in example-2 -----	51
Figure 4.2.c: Illustration of boundaries of example-2-----	52
Figure 4.2.d: 2D thermal conductance and temperature distribution map of example-2-----	52
Figure 4.3.a: Illustration of example-3 -----	54
Figure 4.3.b: Unventilated air cavities of example-3 -----	54
Figure 4.3.c: Illustration of boundaries of example-3-----	55
Figure 4.3.d: 2D thermal conductance and temperature distribution map of example-3-----	55
Figure 4.4.a: Illustration of example-4 -----	57
Figure 4.4.b: Air cavities of example-4-----	58

Figure 4.4.c: Illustration of boundaries of example-4-----	58
Figure 4.4.d: 2D thermal conductance and temperature distribution map of example-4-----	59
Figure 4.5.a: Illustration of example-5 -----	61
Figure 4.5.b: Air cavities in example-5-----	61
Figure 4.5.c: Illustration of boundaries of example-5-----	62
Figure 4.5.d: 2D thermal conductance and temperature distribution map of example-5-----	62
Figure 4.6.a: Illustration of example-6 -----	65
Figure 4.6.b: Unventilated air cavities of example-6 -----	65
Figure 4.6.c: Illustration of boundaries of example-6-----	66
Figure 4.6.d: 2D Thermal conductance and temperature distribution map of example-6-----	66
Figure 4.7.a: Illustration of example-7 -----	69
Figure 4.7.b: Air cavities of example-7.-----	69
Figure 4.7.c: Illustration of boundaries of example-7.-----	70
Figure 4.7.d: 2D thermal conductance and temperature distribution map of example-7-----	70
Figure 4.8.a: Illustration of example-8 -----	72
Figure 4.8.b: Air cavities of example-8.-----	72
Figure 4.8.c: Illustration of boundaries of example-8-----	73
Figure 4.8.d: 2D thermal conductance and temperature distribution map of example-8-----	74
Figure 4.9.a: Illustration of example-9 -----	76
Figure 4.9.b: Unventilated air cavities of example-9 -----	76
Figure 4.9.c: Illustration of boundaries of example-9-----	77
Figure 4.9.d: 2D thermal conductance and temperature distribution map of	

example-9-----	77
Figure 4.10.a: Illustration of example-10 -----	80
Figure 4.10.b: Air cavities of example-10-----	80
Figure 4.10.c: Illustration of boundaries of example-10 -----	81
Figure 4.10.d: 2D thermal conductance and temperature distribution map of example-10 -----	81

List of Tables

Table 3-1: Comparison of analytical and THERM results -----	39
Table 3-2: The centre-pane thermal transmittance values of a two pane IGU-	41
Table 4-1: All materials used in examples -----	45
Table 5-1: Comparison of FE simulation and reference [5] results of examples 1 to 9 -----	83
Table 5-2: Comparison of FE simulation and reference [5] results of example 10 -----	84

Terms, definitions and symbols:

Symbol	Definition	Unit
A	Area	m^2
b	Width (measured at right angles to heat flow direction)	m
d	Depth (measured in plane to heat flow direction)	m
E	Intersurface emittance	—
F	View factor	—
h	Heat transfer coefficient	$\text{W}/(\text{m}^2.\text{K})$
h_a	Convective heat transfer coefficient	$\text{W}/(\text{m}^2.\text{K})$
h_r	Radiative heat transfer coefficient	$\text{W}/(\text{m}^2.\text{K})$
L^{2D}	Two-dimensional thermal conductance or thermal coupling coefficient	$\text{W}/(\text{m}.\text{K})$
l	Length	m
Q	Rate of heat flow	W
q	Density of heat flow rate	W/m^2
R	Thermal resistance	$\text{m}^2.\text{K}/\text{W}$
R_s	Thermal resistance of cavity	$\text{m}^2.\text{K}/\text{W}$
T	Thermodynamic temperature	K
U	Thermal transmittance	$\text{W}/(\text{m}^2.\text{K})$
σ	Stefan-Boltzmann constant	$\text{W}/(\text{m}^2\text{K}^4)$

ε	Emissivity	—
λ	Thermal conductivity	W/(m.K)
λ_{eq}	Equivalent thermal conductivity	W/(m.K)
Ψ	Linear thermal transmittance	W/(m.K)

CEN Comité Européen de Normalisation

CFD Computational Fluid Dynamics

DGUD Double Glazing Unit

DXF Direct Exchange Format

FEA Finite Element Analysis

IGU Insulated Glazing Unit

ISO International Organization for Standard

1. Introduction

Energy efficient fenestration products (e.g. windows, doors and shutters) are crucial to reduce heat losses in buildings. Improving energy conservation in buildings directly reduces heating bills, whilst also cutting carbon emissions. The successive changes in part-L of building regulations tightened energy efficiency requirements [1]-[4], means heat losses through fenestration products have to be reduced further. There is therefore a need to improve the energy efficiency of fenestration products. Computer simulations such as those described in this report have a great potential in the development of energy efficient products. In this respect, the use of calculation codes is crucial in assessing the performance of a design concept. It is possible to identify commercially viable and energy efficient designs using these tools, in that they can assist in ensuring a product complies with building regulations. For an elegant design solution and to fine tune a product, the industry accepted calculation codes are a work-horse.

The overall thermal transmittance (U-value) is a measure ($\text{W/m}^2\cdot\text{K}$) of a fenestration product's thermal insulation performance. It is an indicator to compare like products on a fair and equitable basis. Heat is lost or gained through a fenestration product when there is a temperature difference between indoor and outdoor environments. The smaller the thermal transmittance, the lower the rate of heat flow and higher its ability to reduce heat loss. In order to ensure the calculations are accurately performed, the relevant standard [5]

clearly states:

To ensure the suitability of the calculation programme used, calculations shall be carried out on the examples described in Annex D. The calculated two-dimensional thermal conductance $L2D$ shall not differ from the corresponding values given in Table D.3 by more than $\pm 3\%$. This will lead to an accuracy of the thermal transmittance, U , and the linear thermal transmittance Ψ , of about 5% .

BS EN ISO 10077-2 (reference [5], p3)

A set of 10 example window, door and shutter models together with their thermal analysis data are in reference [5]. Here criteria are presented for the verification of calculation codes and their estimates of thermal transmittance. In this report the results of the calculation code THERM [6] was compared for each cited examples in reference[5]. Three versions (5.2, 6.3 and 7.1) of THERM code were tested at two refinement levels of finite element mesh. This publication was prepared for research purposes and to satisfy the set criterion for THERM code verification requirements.

1.1 Structure of this report

This report is organised into five chapters, with references following at the end.

The reminder of this chapter, being the introduction, will be dedicated to a general overview of finite element procedures with particular attention dedicated to towards its application employing a specific code (THERM [6]).

Chapter 2 presents the classification of heat transfer modes, and simplified methods to analyse air cavities in frames. Additionally, the

equations for one-dimensional heat transfer in a plane wall and a composite panel are presented. Furthermore, the methods to obtain thermal transmittance and linear thermal transmittance values are detailed.

Chapter 3 presents the calculations of the centre-pane thermal transmittance values of an insulation panel and a glazing unit.

Chapter 4 contains verification examples.

Chapter 5 provides conclusions and compares the FE simulation results with Tables D.3 & D.4 of Annex-D, of the appropriate design standard [5].

1.2 Finite element analysis (FEA)

FEA is a numerical technique to find approximate solutions to mathematical models of given engineering problems that usually involve partial differential equations [7]-[9]. It is a very popular engineering analysis tool to assess the performance of a product without physical testing. Informative years of development, it was only used in structural analysis, over time, it has been extended to many other fields such as thermal, fluid-flow and electromagnetic analyses. In the context of heat transfer problems, analytical solutions can be difficult for simple geometric shapes. It is therefore necessary to use Finite Element (FE) techniques for more complex geometries due to difficulties in building analytical models. There are a host of general purpose proprietary FEA tools available; examples are

ANSYS [10], ABAQUS [11], ADINA [12] and HyperWorks [13], CALCULIX [14], which can solve a broad variety of problems. The steady-state heat transfer problems in the fenestration industry do not require a comprehensive array of analysis features. Calculation programs such as THERM [6], Flixo pro [15] and Frame Simulator[16] are very specific to the glazing/fenestration industry. These codes come with user friendly interfaces with few control variables. This enables users to analyse even very complicated models with ease. However, there is always a possibility of erroneous inputs or assumptions giving incorrect results. Hence, it is recommended to verify FEA results, i.e. by means of experimental and/or analytical methods.

FEA involves dividing-up a domain (geometry of a part) into simpler smaller regions called elements, then estimating the behaviour of each element with a set of algebraic equations; finally re-assembling the individual characteristics of each element to estimate the overall characteristics of the entire problem domain. That is, this method is fundamentally a bottom-up solution technique. The reason for splitting the domain into smaller regions is to make the problem more manageable. Thus, primarily the FE code constructs a computer model of an actual solid geometry into an assembly of several finite elements. This process is frequently referred to as *discretization* [17], [18]. A fine mesh often gives a more accurate solution at an increased

computational cost. In general, the FE solution result converges for an increased number of subdivisions. In the following, the background of FE modelling is explained in its simplest form.

1.3 General methodology

FEA process as a whole is comprised of three stages consisting of pre-processing, solution and post-processing. These general steps are common to FEA and independent of the type of analysed problem or solution strategies followed.

1.3.1 Pre-processing

The user constructs a geometry of the part to be analysed. Many FE codes (incl. THERM [6]) have some capacity to build two/three-dimensional geometries and/or can overlay a mesh on a pre-existing CAD file. Pre-processing mainly involves dividing geometry into elements, continuously linked set of smaller regions, connected at discrete points called nodes.

1.3.2 Solving

After specifying model attributes such as boundary conditions and loads etc. the mathematical equations are solved via numerical methods in the solution phase. The nodal unknown values such as temperatures and thermal load are evaluated. The finite element code (THERM [6]) in this case calculates the temperature at nodes and

derives heat-flux in each element [19], [20]. The energy error norm is then calculated and the mesh refined if non-convergence is obtained. This iterative process continues until convergence.

1.3.3 Post-processing

During this phase, with the aforementioned converged results obtained, the code allows examination of the primary temperature field at the nodes and hence heat flux in each of the elements (across the nodes). The particular FE code (THERM [6]) allows plotting of isotherms, flux vectors and constant flux lines etc.

1.4 Calculation programme THERM

THERM [6] was developed by Lawrence Berkeley National Laboratories (LBNL) [21], with the support of US Department of Energy, and distributed free of cost. THERM is a *2D* steady-state heat transfer finite element analysis code. Heat transfer analyses can be broadly classified into two categories: transient and steady-state. In steady-state analyses, the temperature differences and heat-fluxes driving the heat transfer across a body remain constant with time; conversely, these vary when transient analysis is carried out. It is worth mentioning here for completeness that there are other heat analysis codes available (finite difference method based), such as WinIso2D [22], BISCO [23] and HEAT2 [24].

In THERM geometries can be built entirely in the Graphical User Interface (GUI) or imported from external Computer Aided Design (CAD) software. It has a graphical user interface to build, solve and post-process FE models. THERM only follows a two-dimensional Cartesian coordinate system. Points, lines and polygons are created interactively. Almost all CAD softwares (e.g. AUTOCAD [25], SOLIDWORKS [26], TurboCAD [27], PTC Creo [28] etc.) can import or export files in Drawing Exchange Format (DXF). THERM uses pre-existing DXF files as a model kernel (underlay) to overlay geometries and a finite element mesh. Certain steps are mandatory before exporting a CAD model in to THERM. For instance, models of real structures often contain complex features that are superfluous for thermal analyses. Such features should be simplified to achieve a converged FE solution. However, it is seldom straightforward to identify a desired level of simplification that is a correct compromise between actual physical geometry and an FE model.

Heat transfer involves three modes: conduction, convection and radiation. A discussion being provided (§2.1). THERM does not explicitly simulate convection or radiation, but rather are approximated through use of an effective conductivity. This type of analysis is reasonably accurate [29]- [33] provided that convection currents are not significant in the air cavities of window/door frames. THERM lends numerical algorithms from CONRAD [30],

TOPAZ2D[31], FACET [32] to achieve approximate FE solutions. THERM converts geometry into an FE model automatically. It discretizes geometries into quadrilaterals and triangles of varying size and form. The mesh generation process is controlled by the Quad Tree Mesh Parameter (QTMP). THERM automatically generates a mesh when the user assigns a fixed QTMP value, which can be varied between 3 and 12. A larger value results in a smaller size of the largest element and consequently a finer mesh. A default value of 6 is used, which is sufficient in many cases, although use of higher values is not uncommon. A value of 8 or greater places a significantly larger demand on computational resources, and also results in longer solution time. Hence, the option to increase QTMP should only be exercised when solution convergence cannot be attained. The built-in error estimator automatically refines the grid to meet conformity with the user set value. The FE routines compute the parameter *Percentage Error Energy Norm*, which is related to the gradient of heat flux (energy). If this parameter exceeds the user set value, THERM refines the grid in areas with a high rate of change in the heat flux [33]. It uses a default percentage energy norm of 10%, and represents an uncertainty of less than 1% in the estimated heat transfer. Post-processing in THERM is very simple; it has the ability to display isotherms, flux vectors, constant flux lines, colour infrared and colour flux magnitude.

2. Background

Heat is a form of energy that is in transit within a body whenever temperature difference exists. An understanding of heat transfer is fundamental to thermal transmittance. Therefore, here the heat transfer terms directly relevant to the work undertaken are provided. Note that this work is not attempting to explain all the nuances of heat transfer, but rather give a simple description of its mechanisms. Additionally, simplified methods of analysing heat transfer in window frame cavities are also presented.

2.1 Modes of heat transfer

Heat transfer takes place when there is a temperature difference within a material body or between two or more bodies. When a temperature gradient exists in a body, the zeroth law of thermodynamics dictates that heat will spontaneously flow from a higher to a lower temperature zone until thermal equilibrium is established. Heat transfer is classified into three modes: conduction, convection and radiation. More than one mode of heat transfer often takes place in most practical systems.

2.1.1 Conduction

Conduction is heat transfer through molecular vibration and interaction within a body or bodies. This can be quantified with Fourier's law of heat conduction (2-1), which is the cornerstone of

heat transfer. The law states that the rate of heat flow (Q) in an isotropic and homogeneous solid is proportional to the normal temperature gradient $\left(\frac{dT}{dx}\right)$ and to the cross sectional area (A) available for heat flow.

$$Q = -kA \frac{dT}{dx} \quad (2-1)$$

Here k is proportionality constant, and is referred to as thermal conductivity, which indicates how fast heat will flow in given matter. The minus sign follows from the fact that heat flows in the opposite direction on the temperature scale. Thermal conductivity is expressed in *Watt per meter per Kelvin*, and heat-flow is expressed in *Watts*. The thermal conductivity of a material is defined as the quantity of heat transmitted through the unit area and unit thickness of a material in unit time when a unit temperature difference exists between opposite sides under steady-state conditions.

The ratio of heat-flow (Q) normal to the cross sectional area (A) considered is referred to as heat flux or density of heat-flow (q). It is a vector quantity having both direction and magnitude. The equation (2-1) can be written in terms of density of heat flow as follows:

$$q = -k \frac{dT}{dx} \quad (2-2)$$

The thermal conductivity can be measured experimentally. Denoted with the symbol k in the original work of French mathematician and physicist Joseph Fourier [34],[35], and in many famous text books [36]-[38]. There has been a move to use the notation λ in place of k to maintain consistency with the symbols in relevant standard [5], which is the notation which will be used herein.

2.1.2 Convection

Convection is a more complex mode of heat-transfer involving a combination of mechanisms. It is partly due to conduction as well as fluid (gases and liquids) motion. Convection currents are set-up when there is temperature difference between a moving fluid and solid surface; the heat transfer potential increases with speed of a moving fluid. Newton's law of cooling [34] is used to quantify convection. If the environmental temperature of a fluid is T_∞ and the surface temperature is T_w , the rate of heat transfer is proportional to the difference in temperature. This is expressed in terms of density of heat-flow (q) as follows:

$$q = h_a(T_w - T_\infty) \quad (2-3)$$

Here the proportionality constant h_a is referred to as the convection coefficient or film heat transfer coefficient; the higher it is the more rapid is the heat transfer. The units of h_a is *Watt per square metre per Kelvin*, and is a function of parameters such as the rate of moving fluid, viscosity, density, thermal conductivity. Note that thermal conductivity (λ) is a physical property of a matter whereas h_a is not.

2.1.3 Radiation

Radiation heat loss results from the emission of infrared energy. All bodies emit electromagnetic waves and dissipate energy. Radiation heat transfer is essentially a surface phenomenon dependent on the condition of a surface and its temperature. Warmer objects emit electromagnetic waves more rapidly than colder objects. The heat flux of a black body due to thermal radiation is proportional to the fourth power of their absolute temperature (T). The maximum rate at which a body can emit thermal radiation is according to the following:

$$q = \sigma T^4 \quad (2-4)$$

Here σ is a constant equal to 5.67×10^{-08} W/m².K, q is the heat flux and T is the absolute temperature of the body. Electromagnetic wave propagation can occur in a medium or perfect vacuum; in contrast, conduction and convection modes require a medium for

heat-transfer. Increasing surface reflectivity by means of adding coatings to frame surfaces reduce heat loss through radiation. Only an ideal black-body emits radiative energy at the rate of equation (2-4). In reality, all frame and glazing surfaces dissipate heat at a rate that is lesser than that of a black-body. Emissivity (ϵ) is the ratio of energy radiated by a particular body to that of a black-body at the same temperature. The equation (2-4) referred to as the Stefan-Boltzmann law of thermal radiation; the physics involved being exceedingly complex. A cavity in a frame is a collection of distinct surfaces, and it is not always the case that each face will have uniform emissivity. It is mathematically challenging to estimate how radiative effects are imposed on each of these faces. The view factor is a term adopted to deal with these complex formulations, and is used in the treatment of cavities (§2.2.2). Further background of radiation/view factors is of little relevance to work undertaken here. Detailed discussions are provided on laws of Stefan-Boltzmann, Kirchhoff and Lambert in references [36]-[39], which are the foundation of radiation studies.

2.2 Frame cavities

Conduction, convection and radiation occurs in varying amounts within frame cavities, which are usually filled with air. All three modes have a complex dependency with the temperature gradient across the cavity space. Conduction is inversely proportional to cavity

width. Convection is sensitive to cavity geometry and direction of heat-flow. On the other hand, radiative heat transfer is relatively independent of geometry at lower temperatures; it is however dependent on the surface emittance of cavity walls. Conductive and radiative modes are dominant in small cavities. Larger cavities enable greater freedom of circulating air, which also increases convective heat transfer. Isolating cavities into many small pockets prevents the formation of convective air currents.

The rate of heat-transfer by each mode is calculated separately and added together to estimate the total heat transfer in a cavity. Heat transfer can be estimated accurately with calculation codes, which are often Computational Fluid Dynamics (CFD) based numerical codes. The CPU expenses are generally high for a CFD based simulation. Simplified solutions are available that are capable of analysing combined conduction, convection and radiation within air cavities. These can also give comparable results to CFD simulations for simple cavities, provided no significant convection currents are present. THERM [6] is FE method based and can estimate heat transfer in frame cavities using simplified methods in reference [5]. Note that CFD based solutions are recommended for accuracy, especially for complex problems involving convection being the primary mode of heat transfer. In this respect, it is paramount to identify the primary

heat transfer modes. Engineers should judge whether or not it is feasible to apply a simplified procedure to quantify heat transfer. Special purpose calculation codes relevant to glazing systems (e.g. Flixo pro [15] and Frame Simulator [16], WinIso2D [22], BISCO [23] and HEAT2 [24],) are capable of simulating heat transfer by conduction. These estimate heat transfer in frame cavities using simplified methods similar to those adopted by THERM.

Three types of air cavities are classified in reference [5]. There being: unventilated, slightly-ventilated and fully ventilated. A cavity is treated as unventilated if it is sealed or connected to either the exterior or interior by a slit (opening) not greater than 2 mm. When a slit is greater than 2 mm, it is assumed as an open cavity. These are further sub-divided in to either slightly-ventilated or fully-ventilated types. A slit greater than 2 mm but equal to or less than 10 mm is considered as slightly-ventilated, else it is fully ventilated. In simplified procedures, a cavity is treated as a solid material of conductivity being equal to the base thermal conductivity of air, added to the convection and the radiation components. Equivalent thermal conductivity (λ_{eq}) is dependent on parameters such as cavity orientation with respect to heat flow direction, size and shape, surface emissivity and temperature difference across it.

2.2.1 Convective heat transfer coefficient

This section discusses the simplified procedures in reference [5]. Consider a rectangular cavity of dimensions b and d as shown in Figure 2.2.a. The surface boundaries b and d are perpendicular and parallel to the heat flow. The equivalent thermal resistance (R_s) parallel to the direction of heat flow can be found from the equation (2-5).

$$R_s = \frac{d}{\lambda_{eq}} \quad (2-5)$$

Here R_s is the thermal resistance and λ_{eq} is equivalent thermal conductivity of the cavity.

This thermal resistance is equal to the reciprocal of the sum of the radiation and convective heat transfer coefficients.

$$R_s = \frac{1}{h_a + h_r} \quad (2-6)$$

Here h_a & h_r are the convective and radiation heat transfer coefficients.

The convective heat transfer coefficient (h_a) for a cavity of

dimension (b) perpendicular to the heat flow direction is estimated via equation (2-7).

$$\text{If } b < 5 \text{ mm, } h_a = \frac{C_1}{d} \quad (2-7)$$

Here C_1 is a constant and is equal to $0.025 \text{ W}/(\text{m} \cdot \text{K})$

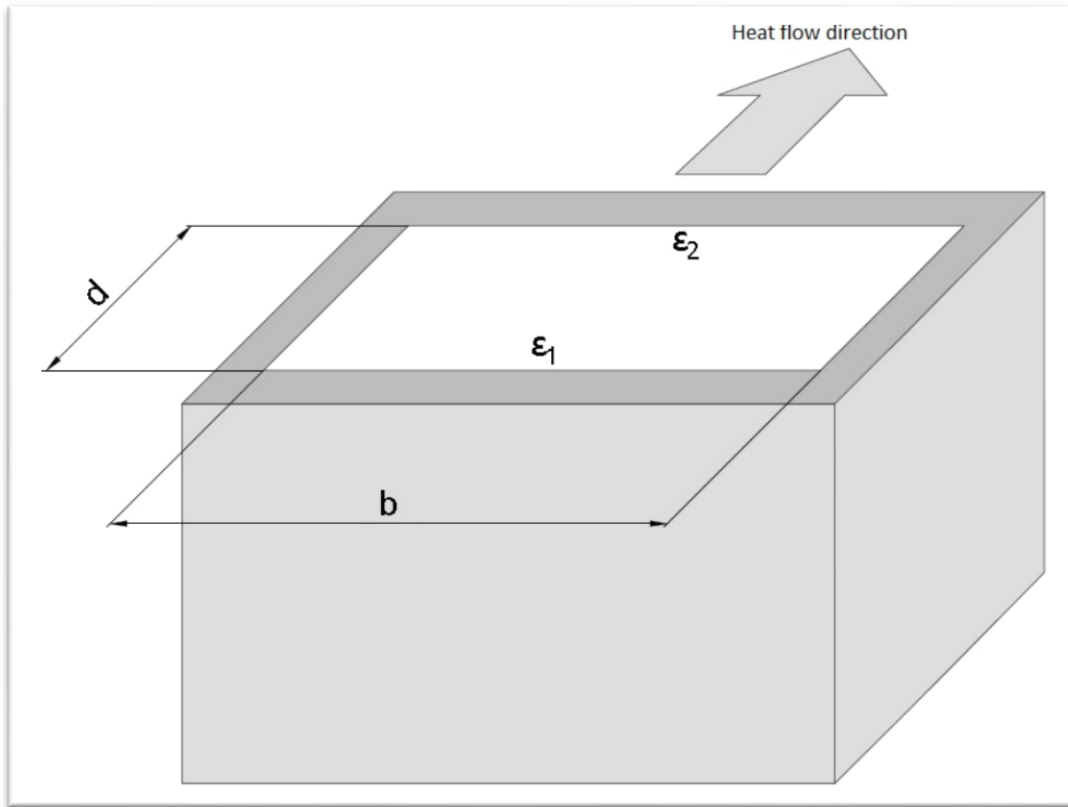


(Image is redrawn from reference [5])

Figure 2.2.a: Illustration of a rectangular cavity

If $b \geq 5 \text{ mm}$, and the surface temperature difference (ΔT) in a cavity is known, the following equation is used:

$$h_a = \max \left\{ \frac{C_1}{d}; C_2 \Delta T^{1/3} \right\} \quad (2-8)$$

Here C_1 is $0.025 \text{ W}/(\text{m} \cdot \text{K})$ and C_2 is $0.73 \text{ W}/(\text{m}^2 \cdot \text{K}^{4/3})$

If no other information is available on the temperature difference (ΔT) in a cavity, it is assumed to be 10K . The convective heat transfer coefficient (h_a) is estimated with the following equation:

$$h_a = \max \left\{ \frac{C_1}{d}; C_3 \right\} \quad (2-9)$$

Here C_3 is $1.57 \text{ W}/(\text{m}^2 \cdot \text{K})$

2.2.2 Radiative heat transfer coefficient

The radiation heat transfer coefficient (h_r) is estimated using equation (2-10) if the mean temperature (T_m) in a cavity is known.

$$h_r = 4\sigma T_m^3 EF \quad (2-10)$$

Here σ is the Stefan-Boltzmann constant, and is equal to $5.67 \times 10^{-8} \text{ W}/(\text{m}^2 \cdot \text{K}^4)$. The parameter E is the intersurface emittance and

F is the view factor. These are estimated for a rectangular section with equations (2-11) & (2-12).

$$E = \left(\frac{1}{\varepsilon_1} + \frac{1}{\varepsilon_2} - 1 \right)^{-1} \quad (2-11)$$

Here ε_1 and ε_2 are the emissivities of internal cavity surfaces in the heat flow direction (see Figure **2.2.a**). The view factor is estimated as follows:

$$F = \frac{1}{2} \left(1 + \sqrt{1 + (d/b)^2} - d/b \right) \quad (2-12)$$

If temperature distribution in a cavity is not known, then the radiation heat transfer coefficient is estimated as follows:

$$h_r = C_4 \left(1 + \sqrt{1 + (d/b)^2} - d/b \right) \quad (2-13)$$

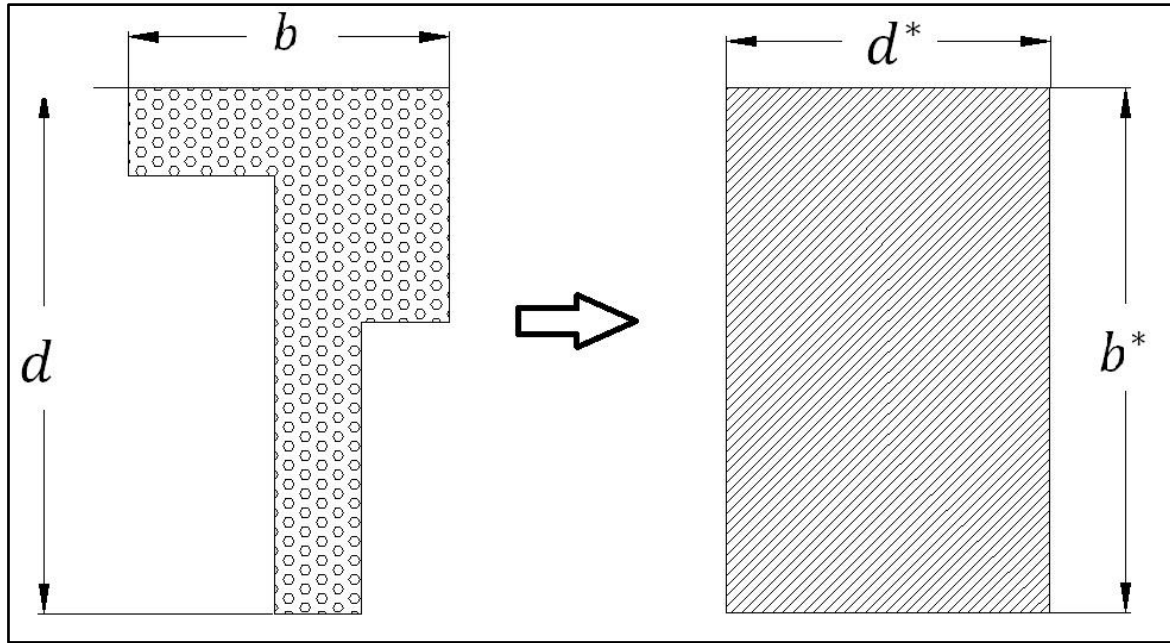
Here C_4 is 2.11 W/(m².K)

The equivalent conductivity of a slightly-ventilated cavity is twice that of an unventilated one of the same size. Therefore, the

analytical method of calculation uses the same simplified equations even for slightly-ventilated cavities, followed by finally doubling the equivalent thermal conductivity. The non-rectangular cavities are converted to equivalent rectangular sections in order to apply simplified equations. In Figure 2.2.b, an illustration is provided on the conversion procedure. A small circumscribing rectangle (total cavity area A) of depth d and width b is converted to equivalent cavity of depth d^* and width b^* . Non-rectangular cavities are always transformed to equivalent rectangles having identical aspect ratio ($d/b = d^*/b^*$) and the same cavity area ($A = A^*$). Here A^* is the area of the equivalent cavity, b^* & d^* are the width and depth of the smallest circumscribing rectangle. The equivalent cavity depth d^* and width b^* is estimated with following equations:

$$b^* = \left(\sqrt{A \frac{b}{d}} \right)^{1/2} \quad (2-14)$$

$$d^* = \left(\sqrt{A \frac{d}{b}} \right)^{1/2} \quad (2-15)$$



(Images are redrawn from reference [5])

Figure 2.2.b: Transformation of a non-rectangular cavity

2.3 One-dimensional steady-state heat transfer

The Fourier law (§2.1.1) is used to analyse one-dimensional heat-flow. It is assumed that the system is in a steady-state, which implies that temperatures remain constant with time. One-dimensional (*1-D*) means the temperature is dependent on one variable (thickness) only. The temperature is considered uniform over the surfaces perpendicular to the heat flow direction. Here, the analytical equations for the thermal transmittance are derived for two cases. The first is a simple plane slab separated by interior and exterior environments, and the second a composite of 3 layers. The second case is further extended to study a two-pane Insulated Glazing Unit (IGU).

2.3.1 Plane slab

The thermal transmittance of a plane slab is derived here from first principles. Figure 2.3.a shows a plane slab exposed to a cooler external temperature (T_{ext}) on one surface boundary and a hot internal temperature (T_{int}) on the opposite (i.e. $T_{ext} < T_{int}$). The surface boundary temperatures on the interior (indoor) and exterior (outdoor) sides are T_2 and T_1 respectively. Heat is exchanged when the surface of a solid material is exposed to fluid, moving air in this case, at a different temperature. Newton's law of cooling has been used to quantify convective heat exchange between a solid body (plane slab) and surrounding air. The net heat flux (q) entering from the hot indoor side is equal to that exiting the cold outdoor side.

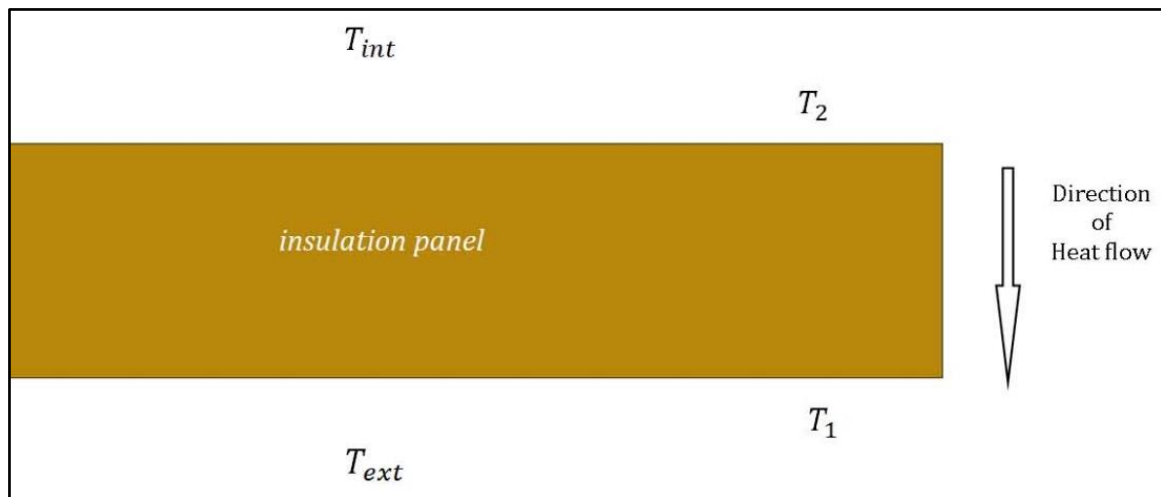


Figure 2.3.a: Illustration of a plane slab

Convection occurs when a body of air at the indoor side comes into contact with the plane slab. It is assumed that the ambient indoor air temperature (T_{int}) is higher than the indoor side surface temperature of the slab. Heat transfers from the indoor to outdoor side within the plane slab via conduction (according to the principles of Fourier law). Finally, heat is exchanged to the cooler outdoor air by convection and/or radiation across the surface of the slab. Therefore, both Fourier's law of conduction and Newton's law of cooling have been used to develop formulations. The heat flux (q) from warm indoor air to the surface of plane slab according to Newton's law of cooling is as follows:

$$q = h_{int,a}(T_{int} - T_2) \quad (2-16)$$

Here $h_{int,a}$ is the convection heat transfer coefficient. Equation (2-16) is a good approximation provided that the radiation mode of heat transfer is negligible. However, heat is also exchanged via radiation. For the purpose of the calculation, the radiation heat transfer law can also be approximated as a linearized form analogous to equation (2-16). The radiation heat transfer coefficient ($h_{int,R}$) is a function of parameters such as temperature, emissivity and absorptivity of surfaces. Since $h_{int,R}$ is not a physical constant like thermal

conductivity; both radiation and convection heat transfer coefficients should be combined to yield an effective heat transfer coefficient. The sum of convection and radiation heat transfer coefficients is then quantified with standard internal heat transfer coefficient (h_i), which is as follows:

$$h_i = h_{int,R} + h_{int,a} \quad (2-17)$$

Here h_i combines both convection and radiation effects with a single parameter. The corrected formulation for the heat flow (q) is:

$$q = h_i(T_{int} - T_2) \quad (2-18)$$

Thus considers the combined effects of both convection and radiation, and can also be written as:

$$T_{int} - T_2 = q \left(\frac{1}{h_i} \right) \quad (2-19)$$

Here, the ratio $1/h_i$ is also referred to as the surface film thermal resistance in $\text{m}^2 \cdot \text{K}/\text{W}$. The net heat entering on the indoor side of the

plane slab is transmitted via conduction. The heat flux (q) within the plane slab, application of equation (2-1) gives:

$$q = \lambda \left(\frac{T_2 - T_1}{d} \right) \quad (2-20)$$

Here, the thermal conductivity of the plane slab is λ and its thickness is d . Equation (2-20) can be re written as follows:

$$T_2 - T_1 = q \left(\frac{d}{\lambda} \right) \quad (2-21)$$

Where heat flux (q) transferred to outdoor air from the surface of a plane wall, taking into account convection and radiation, is given by:

$$q = h_e (T_1 - T_{ext}) \quad (2-22)$$

Here, h_e is the standard external heat transfer coefficient. Equation (2-22) can also be written as follows:

$$T_1 - T_{ext} = q \left(\frac{1}{h_e} \right) \quad (2-23)$$

Combining equations (2-19), (2-21) and (2-23) renders:

$$q = \frac{T_{int} - T_{ext}}{\left(\frac{1}{h_i} + \frac{d}{\lambda} + \frac{1}{h_e} \right)} \quad (2-24)$$

The thermal transmittance is found by adding the thermal resistance of the slab, plus the surface film thermal resistances on each side, and then taking the reciprocal.

The generalized formula for the density of heat-flow in terms of overall thermal transmittance (U-value) can be written as:

$$q = U \Delta T \quad (2-25)$$

Here ΔT is the temperature difference between two environments; $\Delta T = T_{int} - T_{ext}$.

From equations (2-24) and (2-25), the centre-pane thermal transmittance (U-value) of the plane slab is:

$$U = \frac{1}{\left(\frac{1}{h_i} + \frac{d}{\lambda} + \frac{1}{h_e}\right)} \quad (2-26)$$

2.3.2 Composite panel

Here, the equation for the overall thermal transmittance (U-value) of a three layered composite panel is derived. Consider a composite plane wall shown in Figure 2.3.b. It is constructed with three layers each of material thermal conductivities λ_1, λ_2 & λ_3 respectively. The indoor side surface boundary temperature of layer 1 is at T_4 , and is exposed to hot air at T_{int} . The outdoor side surface boundary temperature of layer 3 is T_1 . It is exposed to ambient outdoor air temperature T_{ext} . The intermediate layer is at temperatures T_2 and T_3 , bounding outer and inner layers respectively. Heat is exchanged from hot indoor air to the boundary surface of layer 1. This heat energy travels within the composite panel via conduction before exchanging to the cooler outer air at the boundary surface of layer 3.

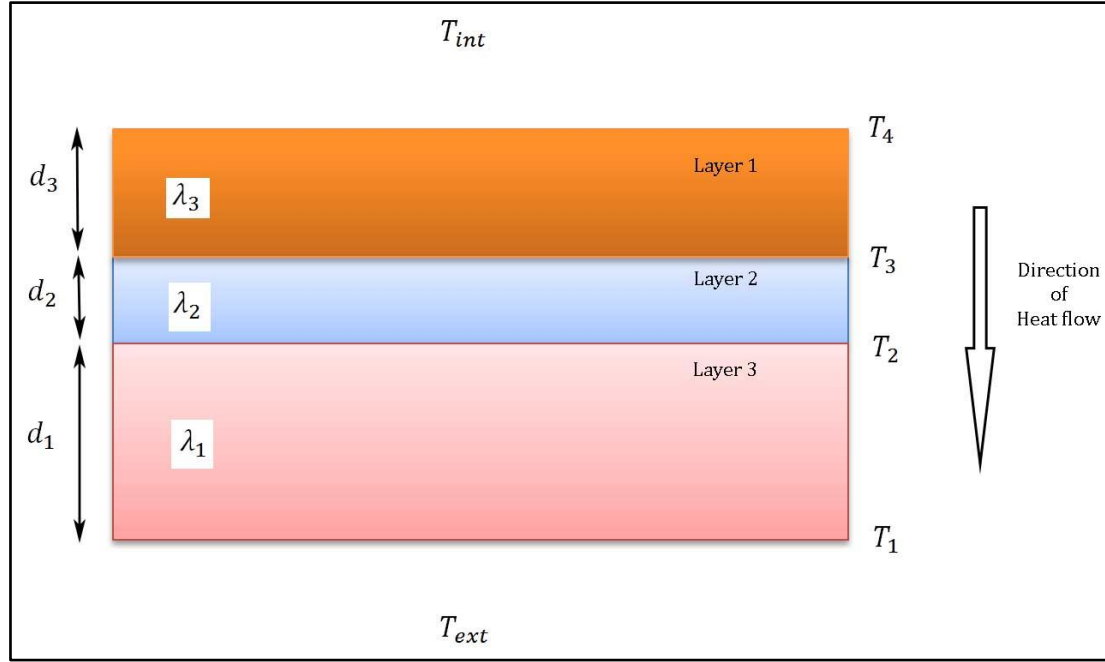


Figure 2.3.b: Illustration of a three layered composite panel

The exposed boundary surfaces of the composite panel on the indoor and outdoor sides are open to a body of air. Thus, mainly the convection mode of heat transfer takes place, in parallel with radiation. The combined effects are captured using heat transfer coefficients h_i & h_e for indoor and outdoor boundary surfaces respectively. The density of heat flow (q) from hot indoor air to the boundary surface of layer 1 is:

$$q = h_i(T_{int} - T_4) \quad (2-27)$$

Here, h_i is the standard internal heat transfer coefficient. Equation (2-27) in terms of temperature difference is:

$$T_{int} - T_4 = q \left(\frac{1}{h_i} \right) \quad (2-28)$$

Heat transfer by conduction within the composite panel is dealt with using Fourier's law. For layers 1, 2 and 3 it is quantified with equations (2-29), (2-30) & (2-31) respectively.

$$q = \lambda_3 \left(\frac{T_4 - T_3}{d_3} \right) \quad (2-29)$$

$$q = \lambda_2 \left(\frac{T_3 - T_2}{d_2} \right) \quad (2-30)$$

$$q = \lambda_1 \left(\frac{T_2 - T_1}{d_1} \right) \quad (2-31)$$

Here d_1 , d_2 & d_3 are the thicknesses of layer 1, 2 and 3 respectively. Equations (2-29), (2-30) & (2-31) can be rewritten in terms of temperature differences in each layer.

$$T_4 - T_3 = q \left(\frac{d_3}{\lambda_3} \right) \quad (2-32)$$

$$T_3 - T_2 = q \left(\frac{d_2}{\lambda_2} \right) \quad (2-33)$$

$$T_2 - T_1 = q \left(\frac{d_1}{\lambda_1} \right) \quad (2-34)$$

The density of heat flow (q) from the outdoor surface of layer 3 to the ambient air is given by:

$$q = h_e(T_1 - T_{ext}) \quad (2-35)$$

Here, h_e is the standard external heat transfer coefficient, it combines both convection and radiation effects.

Equation (2-35) can be re written as follows:

$$T_1 - T_{ext} = q \left(\frac{1}{h_e} \right) \quad (2-36)$$

Combining equations (2-28), (2-32), (2-33), (2-34) and (2-36) and simplifying gives:

$$T_{int} - T_{ext} = q \left(\frac{1}{h_i} + \frac{d_1}{\lambda_1} + \frac{d_2}{\lambda_2} + \frac{d_3}{\lambda_3} + \frac{1}{h_e} \right) \quad (2-37)$$

Equation (2-37) can be rewritten as:

$$q = \frac{T_{int} - T_{ext}}{\left(\frac{1}{h_i} + \frac{d_1}{\lambda_1} + \frac{d_2}{\lambda_2} + \frac{d_3}{\lambda_3} + \frac{1}{h_e}\right)} \quad (2-38)$$

The equation (2-38) can be written in terms of thermal resistances of each layer as follows:

$$q = \frac{T_{int} - T_{ext}}{\left(\frac{1}{h_i} + R_1 + R_2 + R_3 + \frac{1}{h_e}\right)} \quad (2-39)$$

Here R_1 , R_2 and R_3 are thermal resistances of each layer. Overall thermal transmittance (U-value) is found by adding the thermal resistances of all layers of the composite panel, plus surface film thermal resistances on each side, and then taking the reciprocal. In general, the U-value for a multi-panel unit is the reciprocal of the sum total of thermal resistances of all homogeneous layers plus both internal and external surface resistances. A generalized equation for total surface resistance of a composite panel of “n” layers can be written as:

$$R_t = \frac{1}{h_i} + \sum_{i=1}^n \frac{d_n}{\lambda_n} + \frac{1}{h_e} \quad (2-40)$$

Here R_t represents sum total of thermal resistances. Substituting $\Delta T = T_{int} - T_{ext}$, and from equations (2-38) and (2-25), the U-value of the composite panel of three layers can be written as:

$$U = \frac{1}{\left(\frac{1}{h_i} + \frac{d_1}{\lambda_1} + \frac{d_2}{\lambda_2} + \frac{d_3}{\lambda_3} + \frac{1}{h_e} \right)} \quad (2-41)$$

2.4 Surface resistances

Window and doors are commonly exposed to large bodies of air on both exterior and interior surfaces, which induce a degree of resistance to heat flow. Convection is the principal mode of heat transfer for exposed surfaces, with radiation contributing only negligibly for small temperature ranges. Both convection and radiation effects are fashioned with a single surface resistance parameter [5]. Surface resistances are standardized for horizontal, vertical and downward heat-flow directions. However, these surface resistance values in reference [5] are not necessarily the same in actual cases. In practise, the estimation of surface resistances even for simple cases is complex and requires experimental data. Surface resistances are dependent on both material physical characteristics, direction of heat flow and local conditions.

The standardized [5] of surface resistance values for upward, horizontal and downward heat-flows are 0.1, 0.13 and 0.17 m².K/W respectively for the indoor side. It is always 0.04 m².K/W, independent of the direction of heat flow for the outdoor side. A zone of reduced radiation and convection is formed when the boundary surfaces that are parallel and perpendicular to the direction of heat flow meet at a corner. According to the design standard [5], these zones on the indoor side should be assigned with a standard surface resistance of 0.2 m².K/W. For many practical cases involving fenestration products, it is indeed difficult to identify reduced radiation and convection zones precisely. THERM [6] requires the parameter film coefficient (also referred to as heat transfer coefficient), which is the reciprocal of surface thermal resistance. According to the reference [5], the external heat transfer coefficient (h_e) is 25 W/(m².K), and the internal heat transfer coefficient (h_i) for horizontal heat-flow is 7.692 W/(m².K). The heat transfer coefficient is 5 W/(m².K) for zones of reduced influences of radiation and convection.

2.5 Calculation of thermal transmittance

Equations for frame thermal transmittance and the overall heat loss parameter for windows and shutters are provided here.

2.5.1 Windows and doors

The whole product thermal transmittance (U-value) of a window or door is the ratio of the transmission heat loss coefficient (units W.K) to the sum of the areas (units m²) of glazing and frame components ($\sum A_g + \sum A_f$). The transmission heat loss coefficient for the whole product is calculated from:

$$H_t = \sum A_g U_g + \sum A_f U_f + \sum l_g \Psi_g \quad (2-42)$$

Here U_g is the centre-pane thermal transmittance of an IGU; U_f is the thermal transmittance of the frame; Ψ_g is the linear thermal transmittance due to the combined effects of the glazing, spacer and frame. The parameters U_g, U_f & Ψ_g are independent of each other. A_g is the area of the glazing; A_f is the area of the frame; l_g is the total perimeter of glazing, which is the sum total of the visible perimeter of the glass panes. It is possible to calculate whole thermal transmittance (U-value) of any size product so long as the aforementioned parameters are known. The parameters U_f & Ψ_g have to be calculated in two separate simulations for each frame. The frame model is bonded to an insulation panel with a known thermal conductivity in the initial simulation. A schematic is shown in Figure 2.5.a. The

numerical simulation directly provides the 2-*D* thermal conductance of a frame-insulation panel assembly (L_f^{2D}). The frame thermal transmittance (U_f) is then calculated using the following equation:

$$U_f = \frac{L_f^{2D} - U_p b_p}{b_f} \quad (2-43)$$

Here U_p is the thermal transmittance of the insulation panel. The parameters b_p & b_f are the horizontal distances between the sight-line of the insulation panel to the model surface boundaries on the far right and far left respectively.

The linear thermal transmittance (Ψ) calculation involves a second simulation with an Insulated Glazing Unit (IGU). Note that the IGU replaces the insulation panel. A schematic of frame section with an IGU is shown in Figure 2.5.b. Initial simulation provides the U-value of the frame (U_f) and the second directly provides the two-dimensional thermal conductance of the frame-glazing assembly (L_Ψ^{2D}). The linear thermal transmittance (Ψ) value is obtained using the following:

$$\Psi = L_{\Psi}^{2D} - U_f b_f - U_g b_g \quad (2-44)$$

Here U_g is the U-value of the IGU; the dimension b_g is the horizontal distance between the sight-line of the IGU to the point of truncation of the model on the right surface boundary. The dimension b_f is the horizontal distance between the far left surface boundary and the beginning of sight-line of the insulation panel. In many cases, the glass manufacturer provides relevant information on the U_g value. A sample calculation of both L_{Ψ}^{2D} & Ψ parameters are provided in example 10 in (§4).

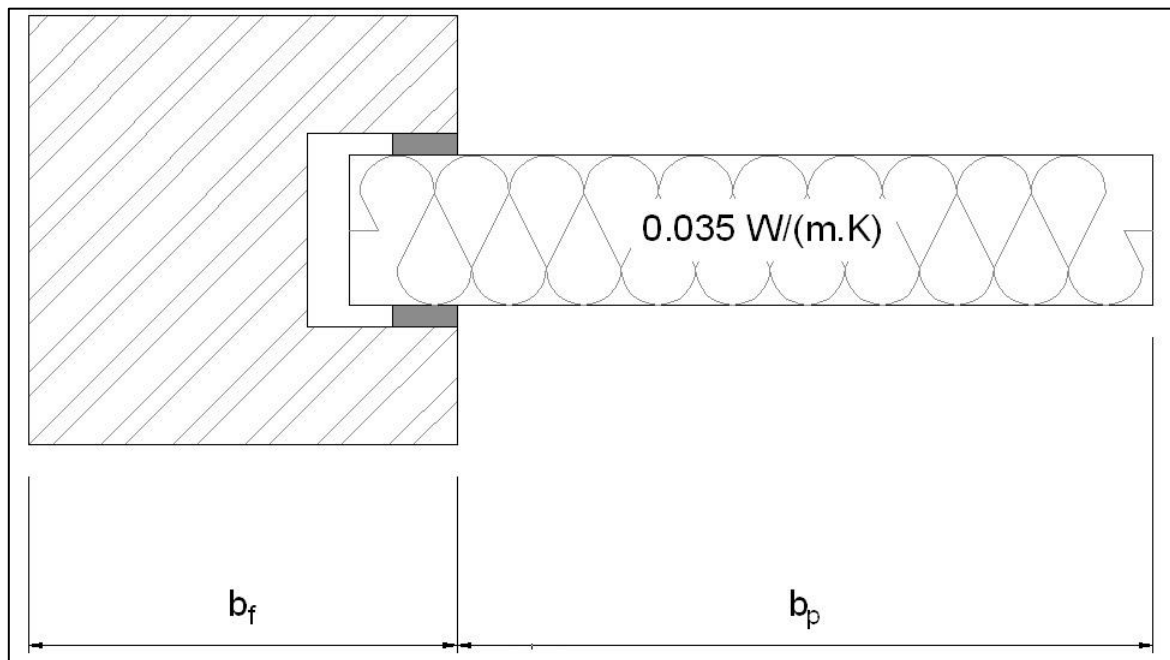


(Image is redrawn from reference [5])

Figure 2.5.a: Schematic of frame section with an insulation panel

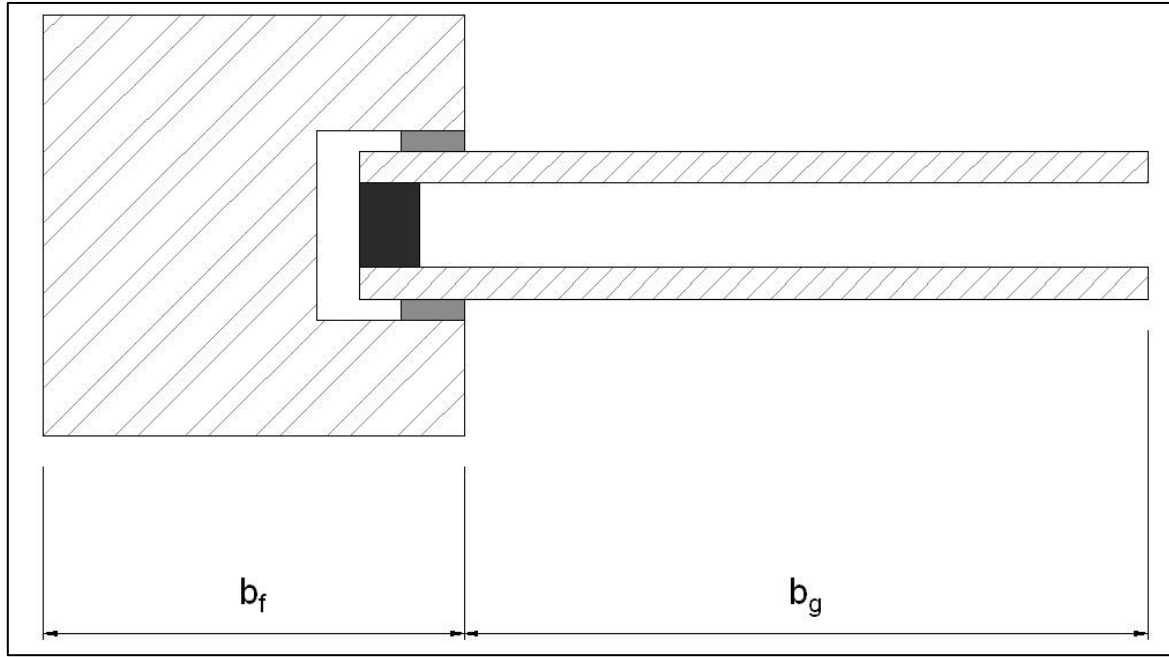


(Image is redrawn from reference [5])

Figure 2.5.b: Schematic of frame section with IGU

2.5.2 Shutters

For shutters the calculation of the thermal transmittance of frame (U_f) is simple as per design standard [5]. It is the ratio of the two-dimensional thermal transmittance (L_f^{2D}) to the height of shutter box (b_{sb}). Thus, the thermal transmittance of shutter frame (U_f) is given by:

$$U_f = \frac{L_f^{2D}}{b_{sb}} \quad (2-45)$$

3. Centre-pane thermal transmittance values

The examples in (§4) require the centre pane thermal transmittance of an insulation panel and/or an Insulated Glazing Unit (IGU) as an input. In this section these are calculated by analytical methods and compared with FE results.

3.1 Insulation panel

The FE simulations in (§4) have used window/door frame models that are bonded to a plane slab of thermal conductivity 0.035 W/m.K . Due to low thermal conductivity, it is referred to as an insulation panel. Here, the thermal transmittance of the insulation panel is calculated for input in the THERM [6] FE code. Four different insulation panels of thicknesses 24, 25, 28 and 58 mm were modelled with the calculation code THERM. The right and left surface boundaries of the model were treated as adiabatic. The top and bottom surface boundaries were modelled with interior and exterior at temperatures of 20 and 0°C respectively. The film coefficients of 7.69 and $25 \text{ W/m}^2\text{.K}$ were assigned to internal and external sides [5]. An Illustration of boundary conditions assigned to the model are shown in Figure 3.1.a. The thermal transmittances as calculated by THERM are compared with analytical calculations in Table 3-1, with perfect agreement demonstrated.

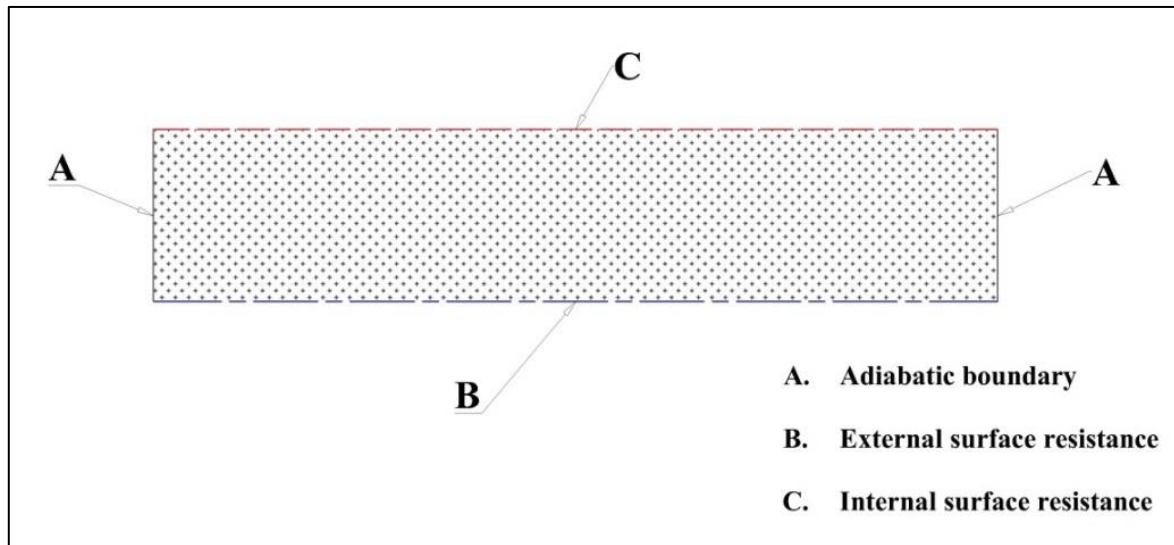


Figure 3.1.a: Illustration of boundary conditions on the insulation panel

Thickness of insulation panel mm	Thermal transmittance $\frac{W}{m^2 K}$	
	Equation (2-26) (Analytical)	THERM (FE method)
24	1.168	1.168
25	1.130	1.130
28	1.030	1.030
58	0.547	0.547

Table 3-1: Comparison of analytical and THERM results

3.2 Two-pane glazing unit

In this section equation (2-41), for a composite panel, is used to obtain the thermal transmittance of a two-pane unit. An Insulated Glazing Unit (IGU) is a composite in nature consisting of two or more panes of glass and insulated gas-spaces. Typically, an IGU is bonded to a window or door frame. Centre-pane thermal transmittance (U-value) is directly dependent on the characteristics of the glass and enclosed gas, and thicknesses. The gas space can be air or a mixture of air with an inert gas filling. Note that when air is replaced with lower thermal conductivity inert gases such as Argon and Krypton the heat transfer features can be further reduced. The thermal conductivity of air is approximately 0.025 W/m.K, whereas it is 0.017 W/m.K for Argon at 20 °C [40]. The references [40], [41] provide a simplified procedure to estimate the heat transfer in an IGU cavity. It involves replacing the cavity by a solid material with an equivalent thermal conductivity that is an approximate of all three modes (viz: conduction, convection and radiation) of heat transfer. In simplified methods, the fill gas is treated as an opaque solid material and assigned an effective conductivity that is equivalent to convection and radiation components plus a base gas material conductivity. This assumption allows the extension of equation (2-41) to the IGU as long as the gas space is sufficiently small such that convection currents do not occur.

3. Centre-pane thermal transmittance values

The example 10 FE model (§4) is constructed with a two-pane IGU and window frame. Its IGU is constructed with 4 mm thick glass separated by a 28 mm wide gas filling. This model was simulated using THERM [6]. A three layered composite plane wall was assigned with a thermal conductivity of 0.034 W/m.K to the central layer, and 1.0 W/m.K for the surrounding two. The heat transfer film coefficients of 7.692 and 25.0 W/m².K were assigned to internal and external surfaces [5]. An illustration of the model is shown in Figure 3.2.a. A perfect agreement between the analytical (using equation (2-41)) and FE results was achieved. The analytical and FE results are in Table 3-2.

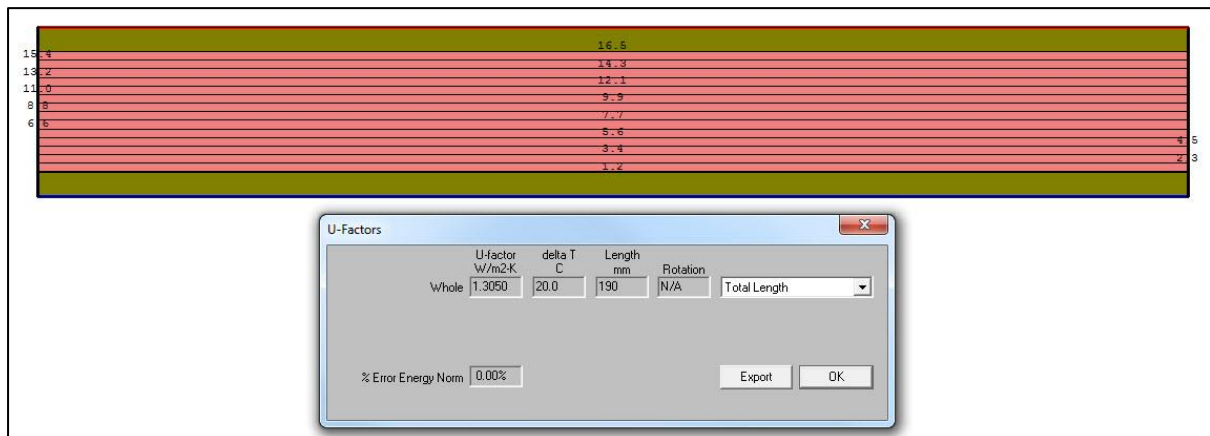


Figure 3.2.a: THERM model of IGU

Thickness (mm)			Thermal conductivity W/m.K			Thermal transmittance $\frac{W}{m^2K}$	
Pane 1 d_1	Gas filling d_2	Pane 2 d_3	Pane 1 λ_1	Gas filling λ_2	Pane 2 λ_3	Analytical	THERM Result
4	20	4	1.0	0.034	1.0	1.305	1.305

Table 3-2: The centre-pane thermal transmittance values of a two pane IGU

4. Computer simulations

The thermal analyses of 10 examples in reference [5] are described here. Simulations were performed with three versions (5.2, 6.3 and 7.1) of THERM [6] code. The 2D thermal conductance (L^{2D}) parameters were directly obtained from an FE analysis. The parameters frame thermal transmittance (U_f) (examples 1 to 9) and the linear thermal transmittance (Ψ) (example 10) were calculated using the equations in (§2.5). The temperature distribution contours are presented for all simulated examples. The operational differences between the three versions of THERM are very little when default settings are kept. Simulations were performed at two different mesh refinement levels. The model geometries were constructed externally with CAD software and exported as a DXF file; these were imported into THERM as an underlay. FE models were constructed in THERM by tracing over the underlay, and using draw and fill functions. Frame cavities were modelled mostly with the fill function in THERM. The cavity definition was set as “CEN”, and larger cavities were split into sub-cavities at throats of 2.0 mm or less. A simplified radiation model in THERM was used with temperature difference of 10°C for all cavities. THERM assumes the cavity fluid to be an equivalent solid and computes the temperatures of cavity walls automatically based on surrounding material temperature. Where necessary the heat-flow directions were adjusted manually. A total of 14 different materials were used, and their thermal conductivity is in Table 4-1.

THERM requires fully defined boundary conditions on all free boundary surfaces. When the *draw boundary conditions* button is selected, THERM automatically sets free surface boundaries to adiabatic conditions. This boundary condition was manually updated to other types where necessary. Adiabatic boundary conditions were assumed as default if no others were explicitly assigned. A maximum of 4 different types of boundary conditions were assigned for free surface boundaries. These being; 1, Adiabatic boundary; 2, External surface resistance; 3, Increased surface resistance, also referred to as reduced radiation/convection, and 4, Internal surface resistance.

- (1) Adiabatic surfaces allow no heat transfer. This is the default boundary condition THERM initially generates.
- (2) The second type of boundary conditions was set to a constant temperature of 0°C with a surface resistance of $0.04 \text{ m}^2\text{K/W}$.
- (3) The third type was assigned only to certain segments of the interior boundary. A temperature of 20°C and a surface resistance of $0.20 \text{ m}^2\text{K/W}$ was assigned.
- (4) The remaining length of boundary not covered by the above was assigned a surface resistance of $0.13 \text{ m}^2\text{K/W}$ and a temperature of 20°C .

The surface resistance parameter is different for the aforementioned 3 and 4 boundary conditions even though both were kept at the same temperature (20°C). To accommodate these two slightly different types, the interior side boundary surface was subdivided at specific locations. Adding new points is the common method to break a surface boundary. The U-factor tag named *Whole* was assigned to the entire interior side boundary surface. That is, to all the surfaces assigned with boundary conditions 3 and 4. Note that the selection of the name *Whole* is entirely arbitrary. The solving process in THERM is straight forward when the model is completely defined. THERM populates the finite element mesh and conducts simulations when the *Calc* button is hit. The numerical routines in THERM store information about temperature and heat transfer parameters for each element of the perimeter. When the *Show U-factors* button is selected after the simulation, THERM directly gives the *2D* thermal conductance of the entire boundary selected as the U-factor tag. Finally, the results were inspected for appropriateness of the model. The patterns of isotherms and flux vectors were examined in addition to the verification of the *2D* thermal conductance parameter. Note that frame cavity results were obtained using *Simplified radiation* models for the examples simulated here.

4. Computer simulations

Key	Material	Thermal conductivity, λ $W/(m \cdot K)$
a	Insulation panel	0.035
b	Soft wood	0.13
c	PVC	0.17
d	EPDM	0.25
e	Polyamide 6.6 with 25% glass fibre	0.30
f	Glass	1.00
g	Steel	50
h	Aluminium	160
i	Pile weather stripping (polyester mohair)	0.14
k	Polyamide	0.25
l	PU (polyurethane), rigid	0.25
m	Polysulfide	0.40
n	Silica gel (dessicant)	0.13
o	Gas filling	0.034 ^a
^a Equivalent thermal conductivity of the gas filling		

(All data in the above are from reference [5])

Table 4-1: All materials used in examples

4.1 Example-1

A thermally broken aluminium frame is shown in Figure 4.1.a. This is the first example in annex-D of reference [5]. The frame is constructed with two separate aluminium extrusions (exterior and interior sides) that are separated by polyamide struts. A 190 mm insulation panel with a thermal conductivity of 0.035 W/m.K is fitted to the frame. The frame is thermally broken through polyamide struts that are strategically placed in-between exterior and interior sections. Polyamide struts interrupt continuity of the aluminium frame impeding the heat transfer via conduction mode. Polyamide is an excellent insulator with a low thermal conductivity of 0.25 W/m.K [5]. Traditionally, aluminium is a preferred choice in industry due to its ability to be extruded to form complex shapes. Aluminium accepts a wide range of coatings. However, due to the highly conductive nature, aluminium frames require thermal breaks. The FE model was constructed with four different materials. The model consists of many unventilated and one slightly-ventilated type air cavities as shown in Figure 4.1.b. Four different types of boundary conditions were assigned to the model as shown in Figure 4.1.c. The surface boundaries exposed to indoor and outdoor environments are shown in red and blue broken lines respectively. The increased surface resistance boundaries are shown in green, and adiabatic in black continuous lines. The thermal transmittance of the 28 mm thick

insulation panel (U_p) separated by exterior and interior environments was calculated previously (see Table 3-1). The FE simulation provided the $2D$ thermal conductance (L_f^{2D}), the model's detailed temperature distribution is plotted in Figure 4.1.d.

For a Quad Tree Mesh Parameter of 7, L_f^{2D} is 0.5599 W/m.K. The thermal transmittance of the insulation panel (U_p) is 1.03 W/m².K. The parameter b_p is the distance between the sight-line of the insulation panel to the surface boundary at the top. Note that as per design standard relevant [5], the length of the panel has to be at least 190 mm measured from the most protruding part of the frame, ignoring any protruding gaskets(s). The parameter b_f is taken as the distance between the bottom surface and the beginning of sight-line of the insulation panel. The parameters b_f and b_p of the current FE model are 110 and 190 mm respectively. The thermal transmittance of frame (U_f) is equal to 3.31 W/m².K (as per the equation (2-43)).

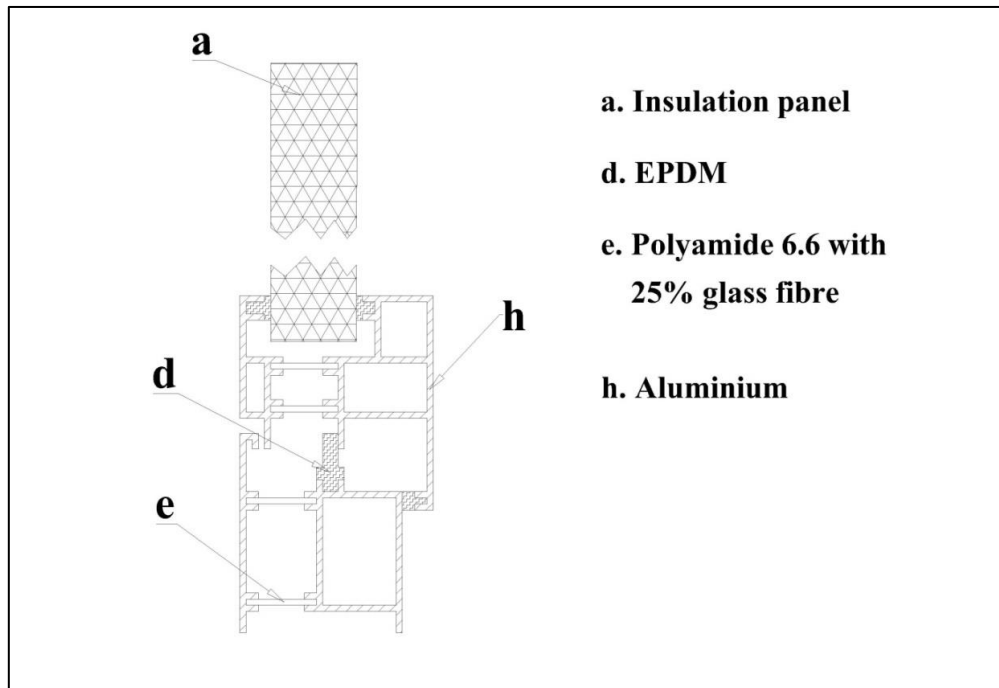


Figure 4.1.a: Illustration of example-1

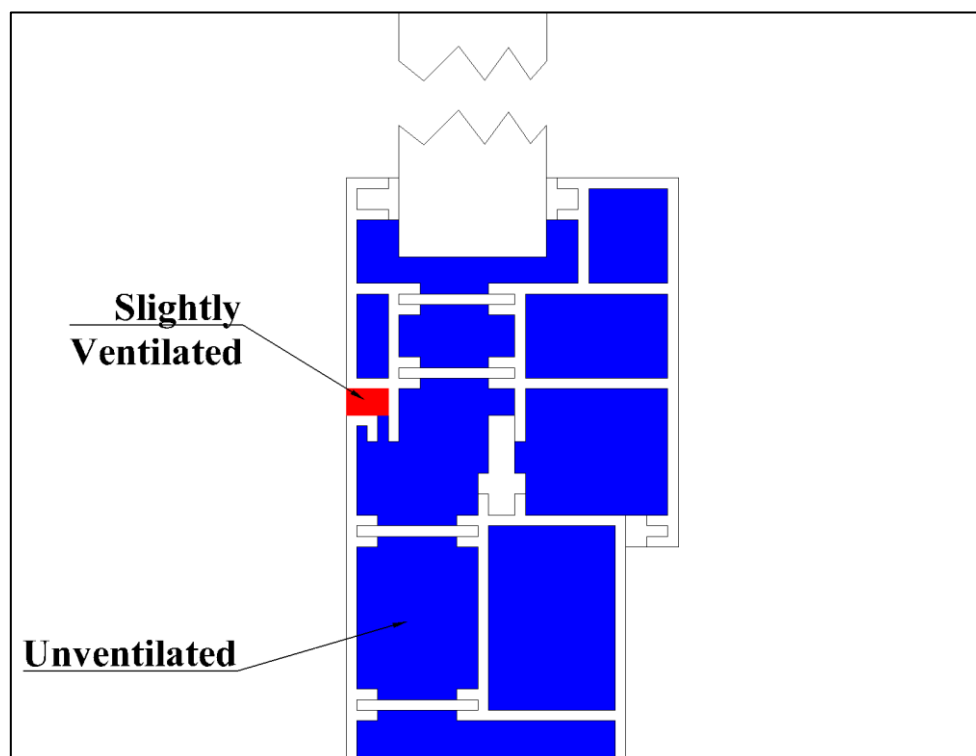


Figure 4.1.b: Air cavities of example-1

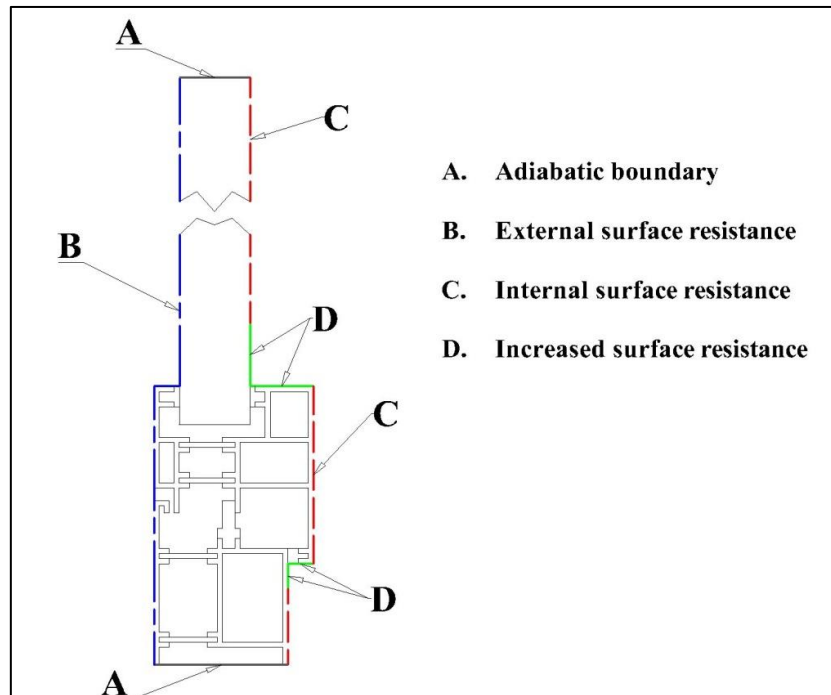


Figure 4.1.c: Illustration of boundaries of example-1

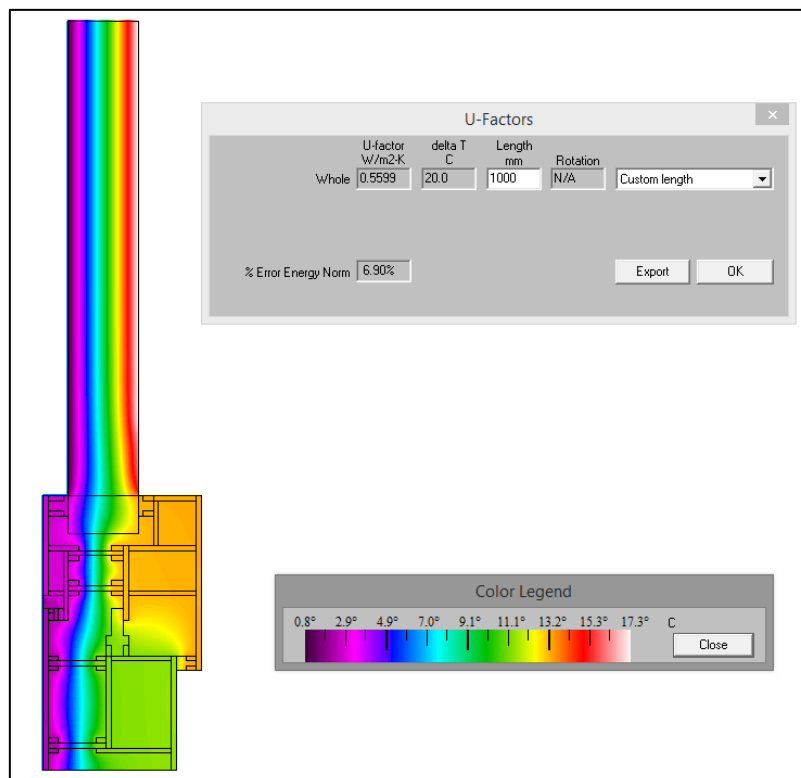


Figure 4.1.d: 2D thermal conductance and temperature distribution map of example-1

4.2 Example-2

An aluminium clad wooden frame section and insulation panel is shown in Figure 4.2.a, which is redrawn from the second example in reference [5]. The exterior surfaces are made of aluminium and the interior with wood. This type of design allows longevity and in many cases easy maintenance. The exterior aluminium surface acts as a weather resistant and protective shield. Being a natural heat insulator, the interior wood reduces heat losses. The frame in Figure 4.2.a is bonded to an insulation panel. The length of the insulation panel modelled in the simulation was 190 mm. In this case all cavities were unventilated shown in Figure 4.2.b. Boundary conditions assigned to the model are shown in Figure 4.2.c. The thermal transmittance (U -value) of the 58 mm thick insulation panel (U_p) is $0.547 \text{ W/m}^2\text{.K}$ (see Table 3-1). The simulation provided the two-dimensional thermal conductance (L_f^{2D}) as shown in Figure 4.2.d. For a Quad Tree Mesh Parameter of 7, L_f^{2D} is 0.2630 W/m.K . The thermal transmittance of the insulation panel (U_p) is $0.547 \text{ W/m}^2\text{.K}$. The parameters b_f and b_p of the model are 110 and 190 mm respectively; b_p & b_f are the distances between the sight-line of the insulation panel to the bottom and top surfaces of the model. The thermal transmittance (U_f) is $1.446 \text{ W/m}^2\text{.K}$ (as per the equation (2-43)).

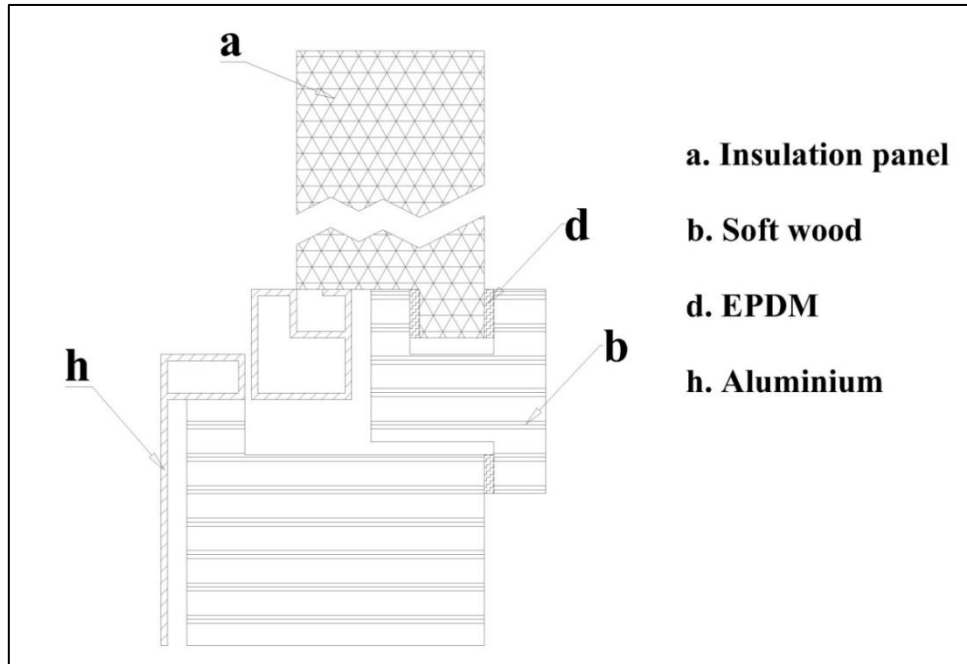


Figure 4.2.a: Illustration of example-2

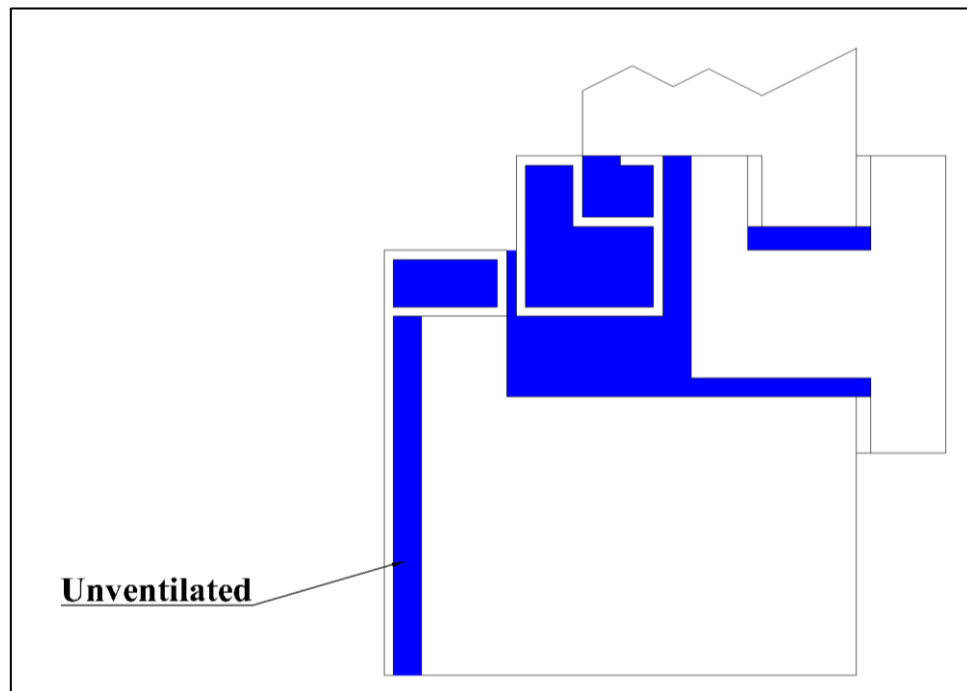


Figure 4.2.b: Unventilated air cavities in example-2

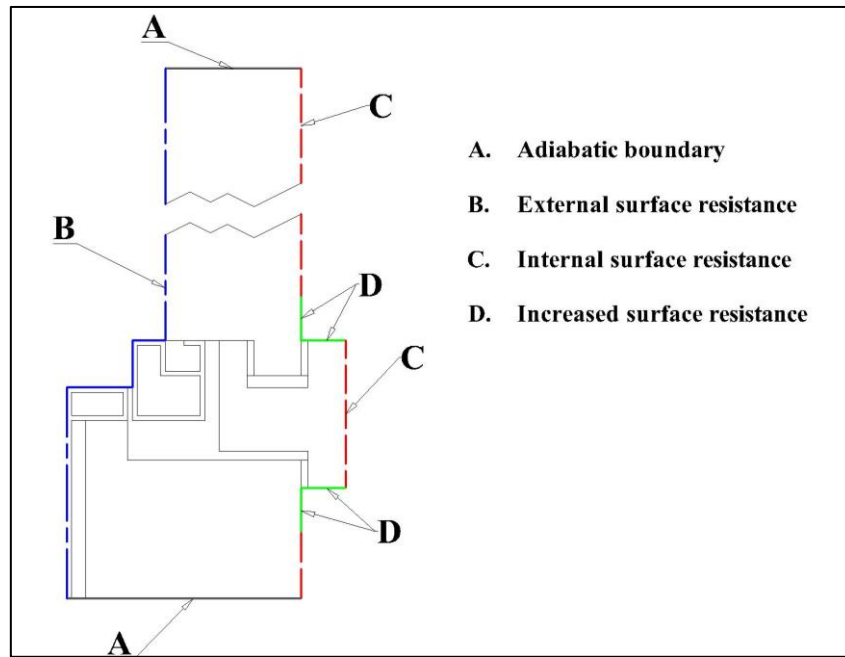


Figure 4.2.c: Illustration of boundaries of example-2

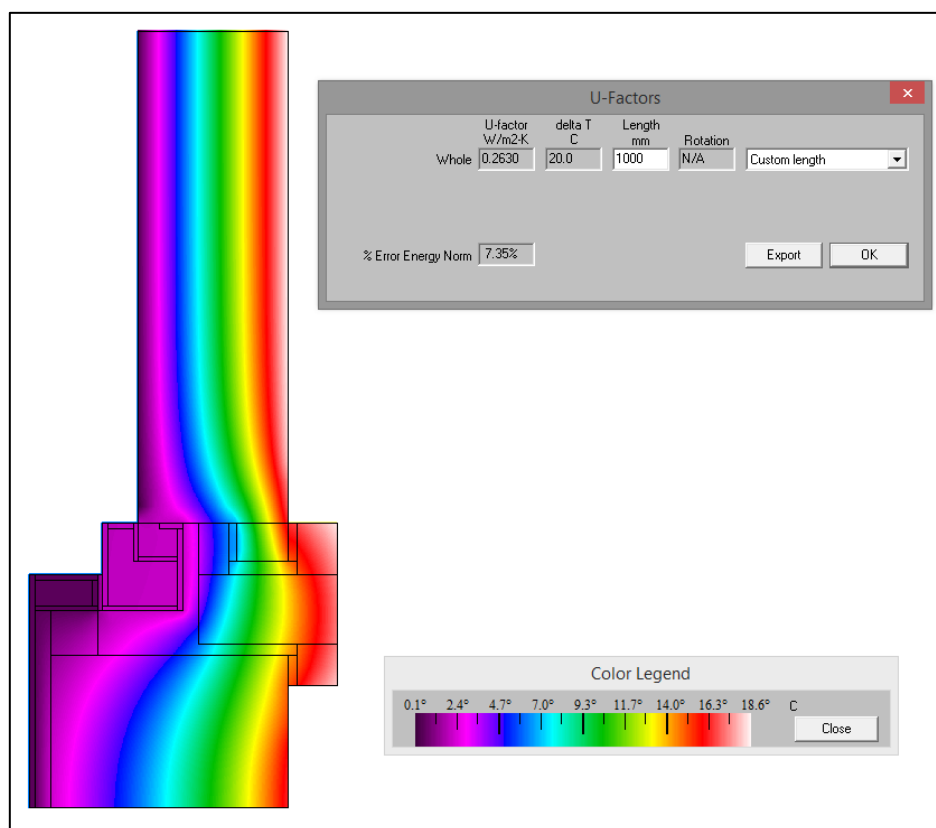


Figure 4.2.d: 2D thermal conductance and temperature distribution map of example-2

4.3 Example-3

A Polyvinyl chloride (PVC) frame section with steel reinforcement and an insulation panel is shown in Figure 4.3.a. This model is redrawn from the third example in reference [5]. This model consists of four different materials. PVC reduces heat losses due to its low thermal conductivity. However, PVC requires additional reinforced supports to prevent distortion. Metals such as steel and aluminium are commonly used as reinforcements. Steel is preferred due to its greater structural strength, lower thermal conductivity and thermal expansion. PVC window frames are always constructed of various sized chambers. Increasing the number of chambers improves thermal insulation features. However, a smaller size chamber also reduces the ability to insert larger metal reinforcements. Hence, there is a trade-off between the size of a metal insert that can be added and the total number of chambers. The unventilated air cavities in the frame are shown in Figure 4.3.b. The four different types of boundary conditions assigned to the FE model are illustrated in Figure 4.3.c.

The thermal transmittance of the 28 mm thick insulation panel (U_p) is $1.03 \text{ W/m}^2\text{.K}$ (see Table 3-1). The simulation computed the 2D thermal conductance (L_f^{2D}) equal to 0.4256 W/m.K (illustrated in Figure 4.3.d). Parameters b_f and b_p are 110 and 190 mm respectively; b_p & b_f are the distances between the sight-line of the

insulation panel to the top and bottom surfaces of the model. The thermal transmittance (U_f) is $2.09 \text{ W/m}^2\cdot\text{K}$ (equation (2-43)).

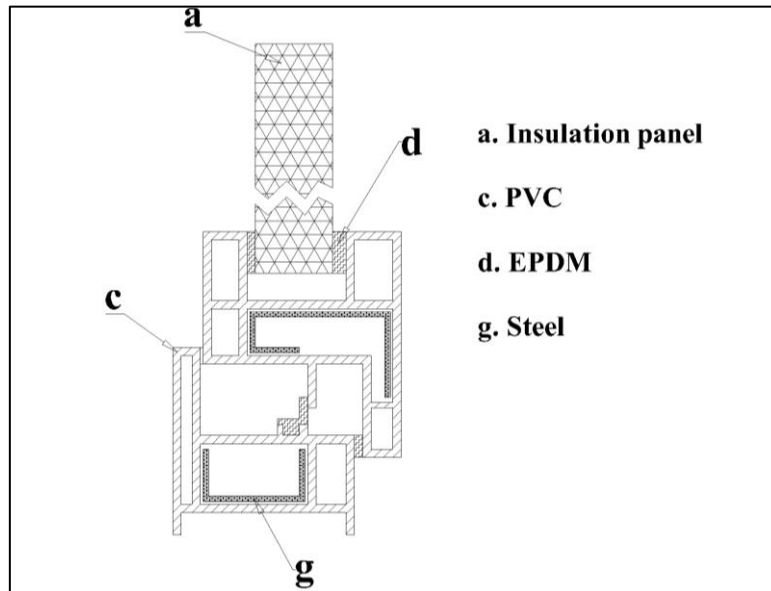


Figure 4.3.a: Illustration of example-3

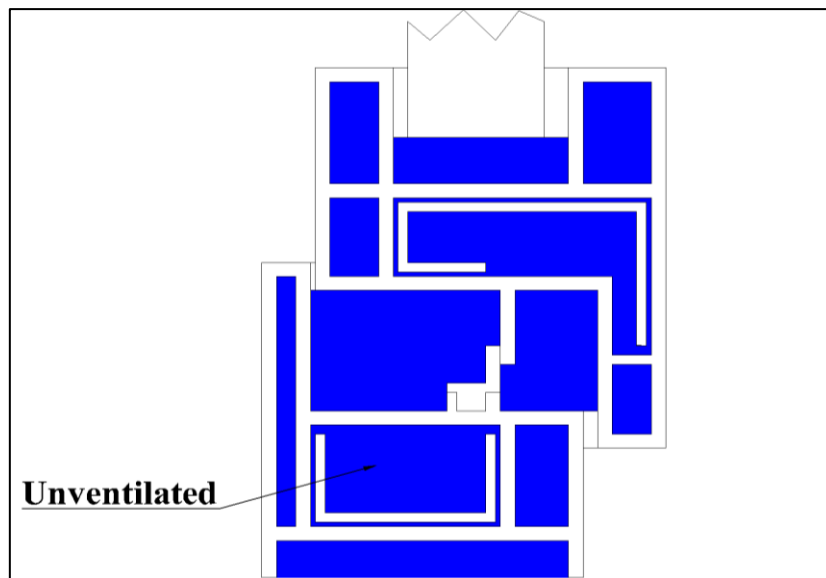


Figure 4.3.b: Unventilated air cavities of example-3

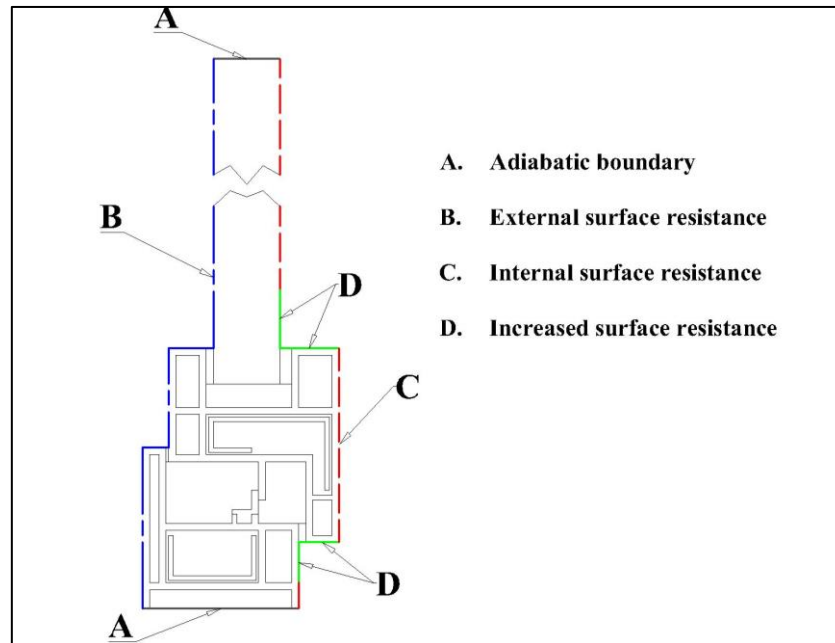


Figure 4.3.c: Illustration of boundaries of example-3

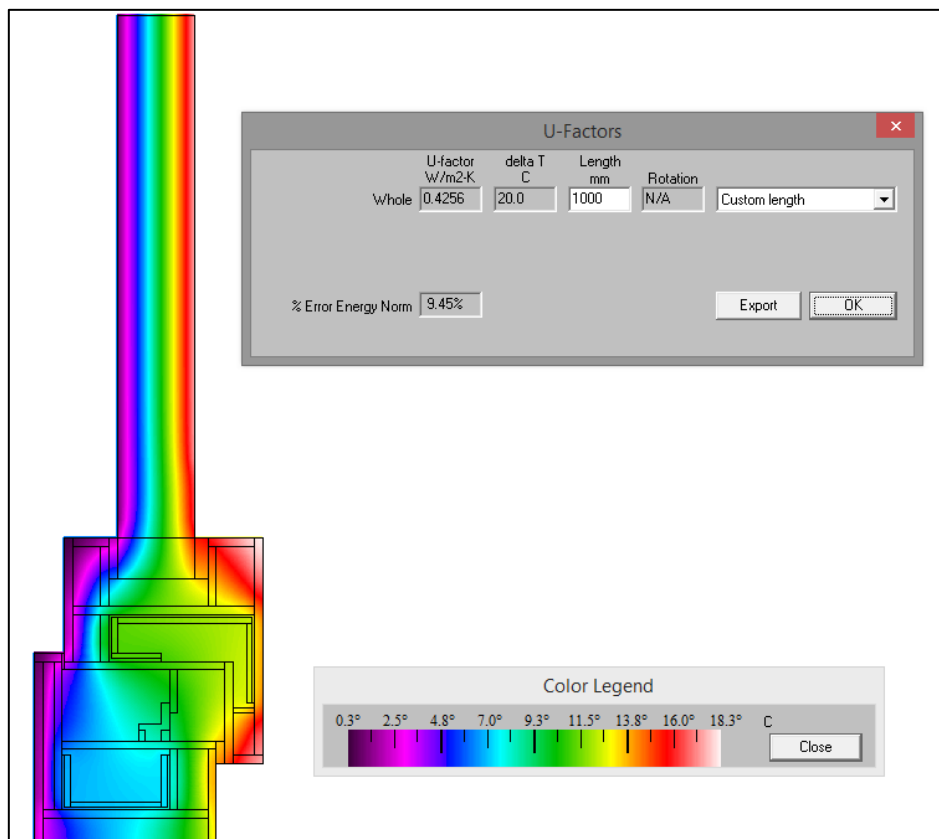


Figure 4.3.d: 2D thermal conductance and temperature distribution map of example-3

4.4 Example-4

The wooden frame section and insulation panel is shown in Figure 4.4.a. This is the fourth example in reference [5]. Essentially, the frame section is constructed with two wooden blocks. Wood is reasonably stiff and yet lightweight owing to its cellular structure, and thus an ideal construction material. Furthermore, it is a natural insulating material with low thermal conductivity. However, the main disadvantage is that it requires protection against weather, wear and tear, moisture and pests. So there are trade-offs of lower utility bills vs. future maintenance costs.

The FE model in Figure 4.4.a is constructed with three different materials. The frame encloses unventilated air cavities of 5 and 6 mm wide, and a slightly ventilated cavity of 5 mm, as shown in Figure 4.4.b. The boundary conditions assigned to the FE model are illustrated in Figure 4.4.c. The thermal transmittance of the 28 mm insulation panel (U_p) separated by exterior and interior environments was $1.03 \text{ W/m}^2\text{.K}$ (Table 3-1). The 2D thermal conductance (L_f^{2D}) was obtained via an FE simulation. The temperature distribution of the simulated FE model is shown in Figure 4.4.d. The calculation to obtain U_f is detailed in the following.

For a Quad Tree Mesh Parameter of 7, L_f^{2D} is 0.3467 W/m.K.

The thermal transmittance of the insulation panel (U_p) is 1.03 W/m².K.

The parameters b_f and b_p in the FE model are 110 and 190 mm respectively; b_p & b_f are the distances between the sight-line of the insulation panel to the top and bottom surfaces of the model. The thermal transmittance (U_f) is 1.3727 W/m².K as per the equation (2-43).

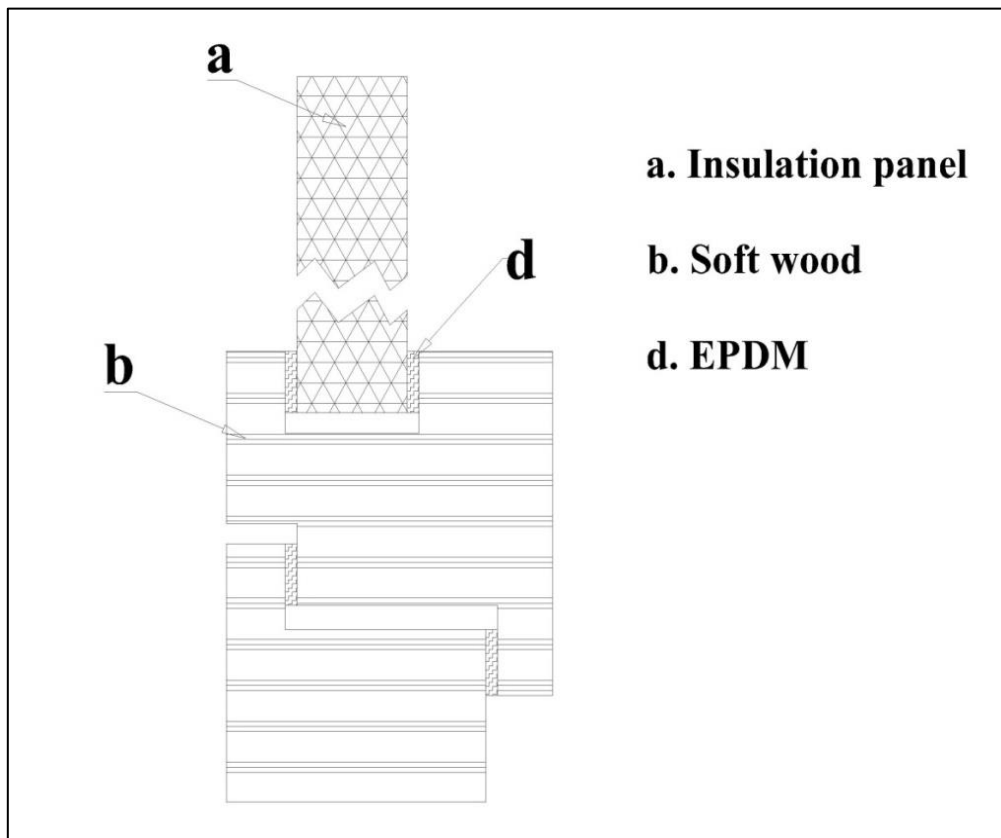


Figure 4.4.a: Illustration of example-4

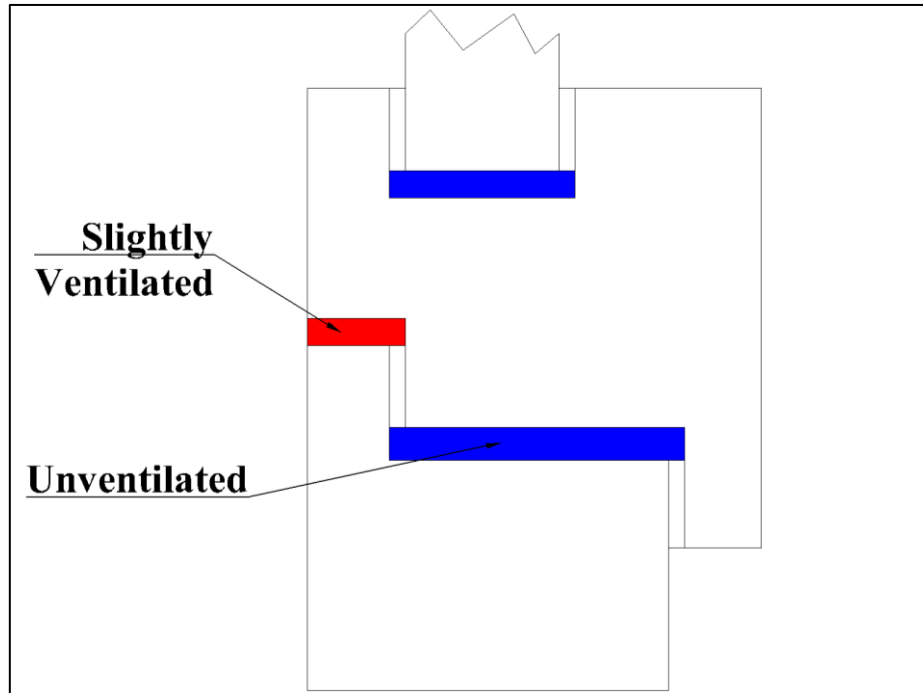


Figure 4.4.b: Air cavities of example-4

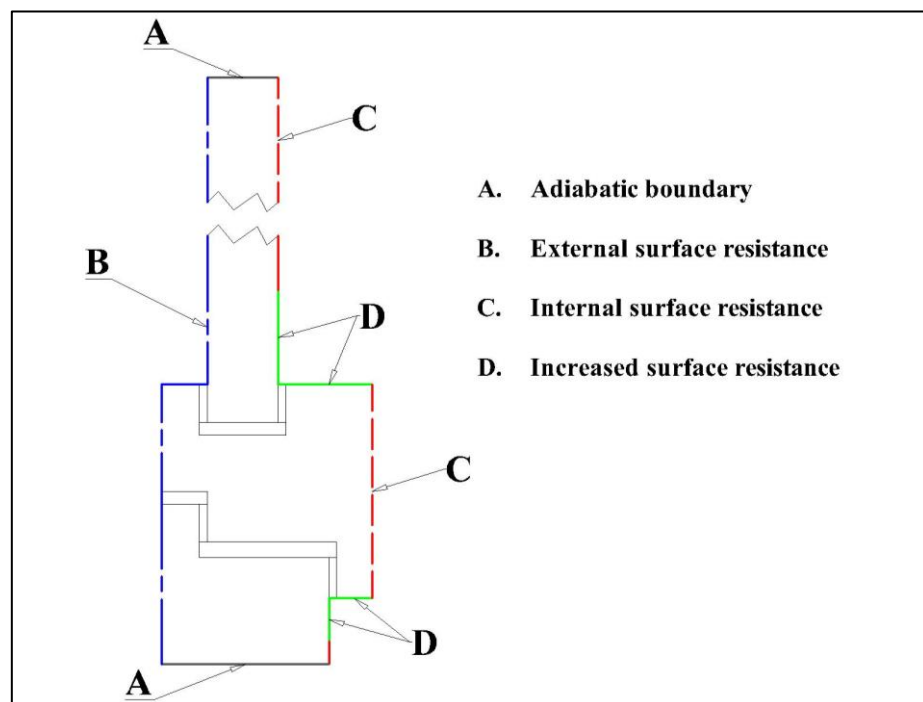


Figure 4.4.c: Illustration of boundaries of example-4

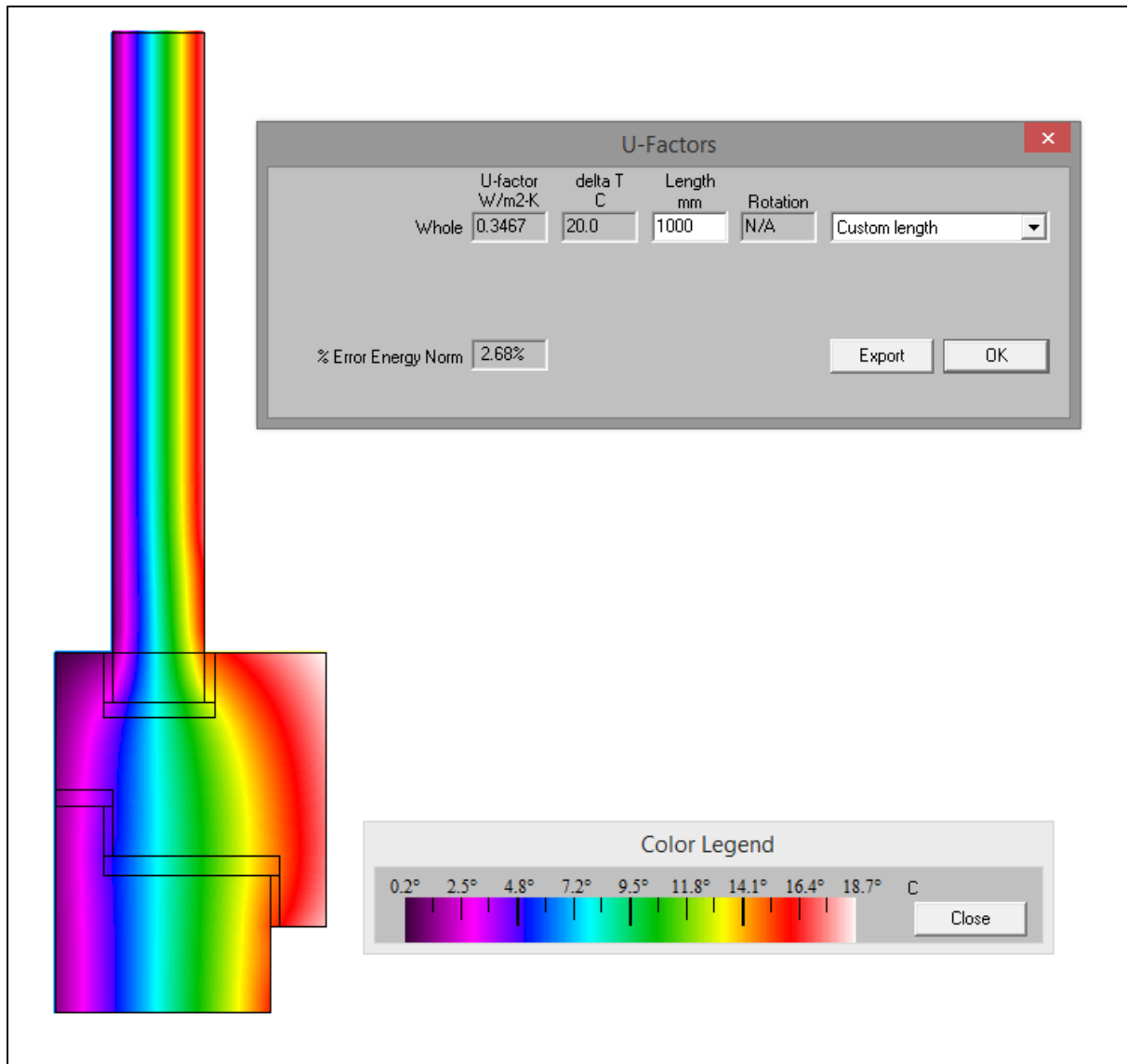


Figure 4.4.d: 2D thermal conductance and temperature distribution map of example-4

4.5 Example-5

A roof window frame section and insulation panel is shown in Figure 4.5.a. This is the fifth example in annex-D of the standard under consideration here [5]. A roof window allows natural light into indoor spaces reducing the need for artificial lighting. Roof windows can be opened (usually via swinging mechanical system) to allow in fresh air. When closed they provide required air tightness, and only allow day light. The roof window frame shown in Figure 4.5.a is constructed with four different types of materials. All unventilated and slightly-ventilated type air cavities in frames are shown in Figure 4.5.b. An illustration of boundary conditions assigned to the FE model is also shown in Figure 4.5.c. The thermal transmittance of 24 mm thick insulation panel (U_p) is $1.168 \text{ w/m}^2\text{.K}$ (see Table 3-1). The $2D$ thermal conductance (L_f^{2D}) and detailed map of temperature distribution of the FE model are shown in Figure 4.5.d.

For a Quad Tree Mesh Parameter of 7, L_f^{2D} is 0.4116 W/m.K .

The parameters b_f and b_p in the FE model are 89 and 190 mm respectively; b_p & b_f are the distances between the sight-line of the insulation panel to the top and bottom surfaces of model. The thermal transmittance (U_f) is $2.1312 \text{ W/m}^2\text{.K}$ as per the equation (2-43).

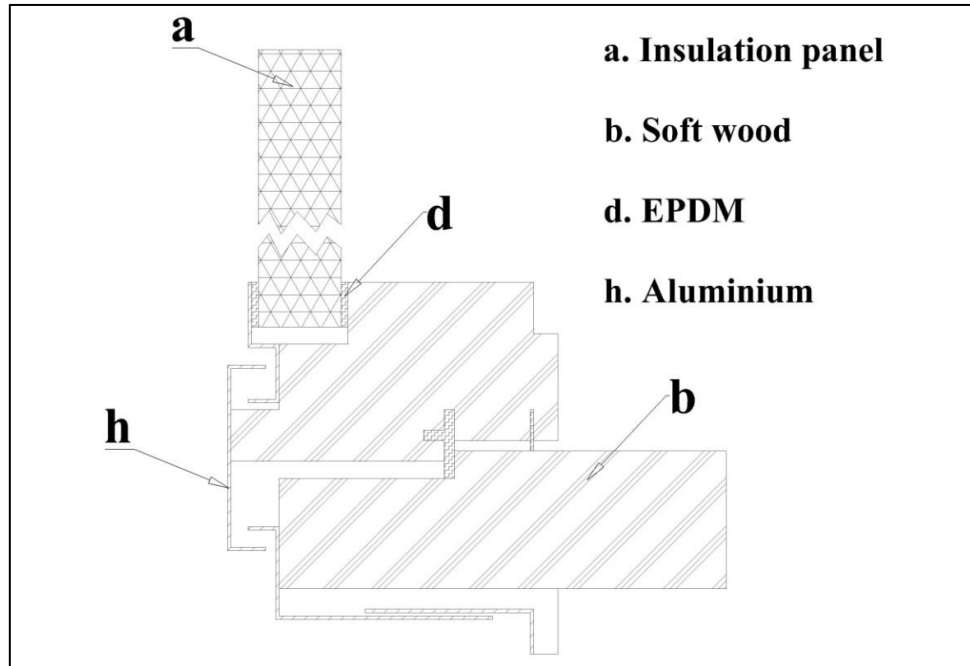


Figure 4.5.a: Illustration of example-5

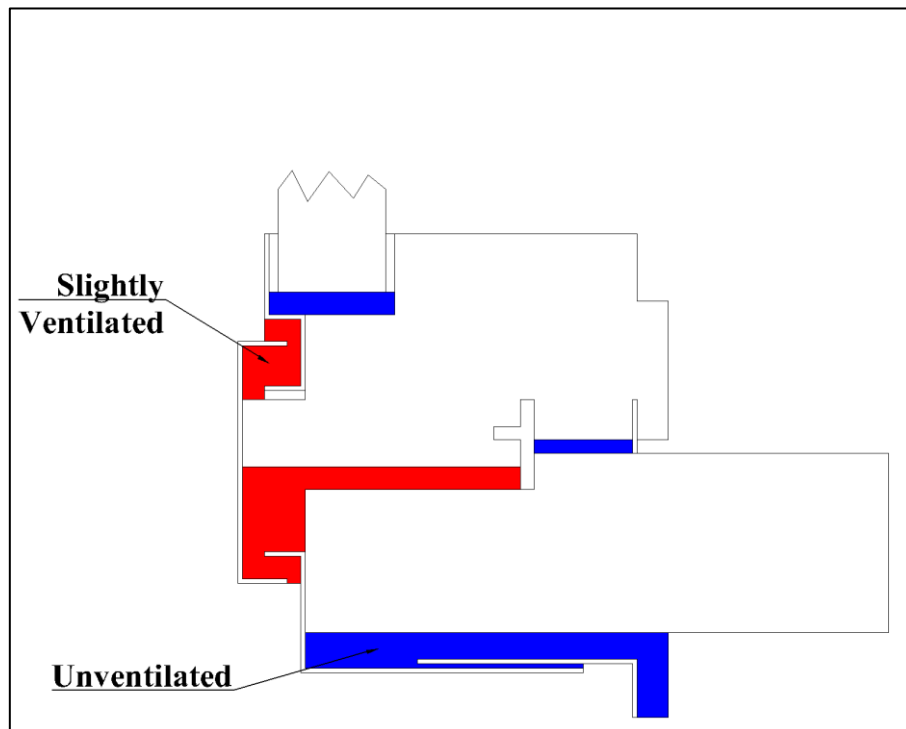


Figure 4.5.b: Air cavities in example-5

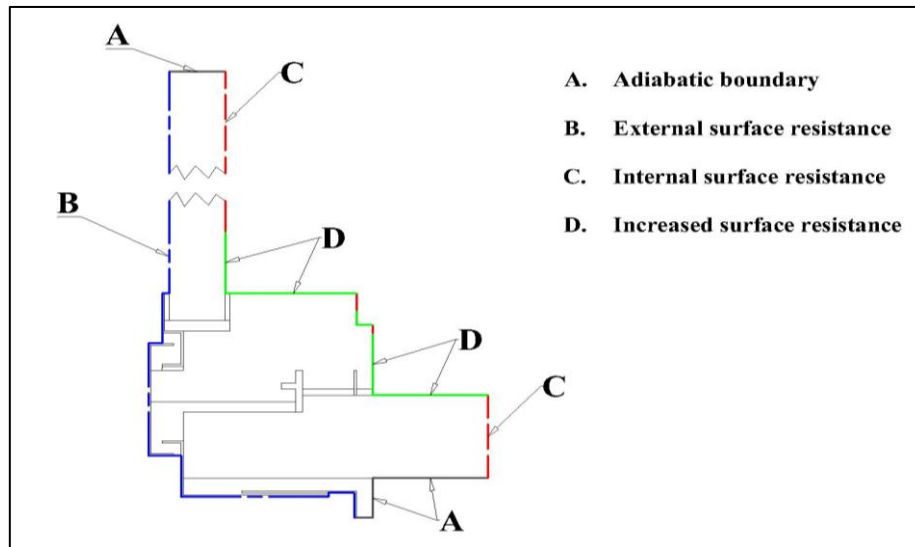


Figure 4.5.c: Illustration of boundaries of example-5

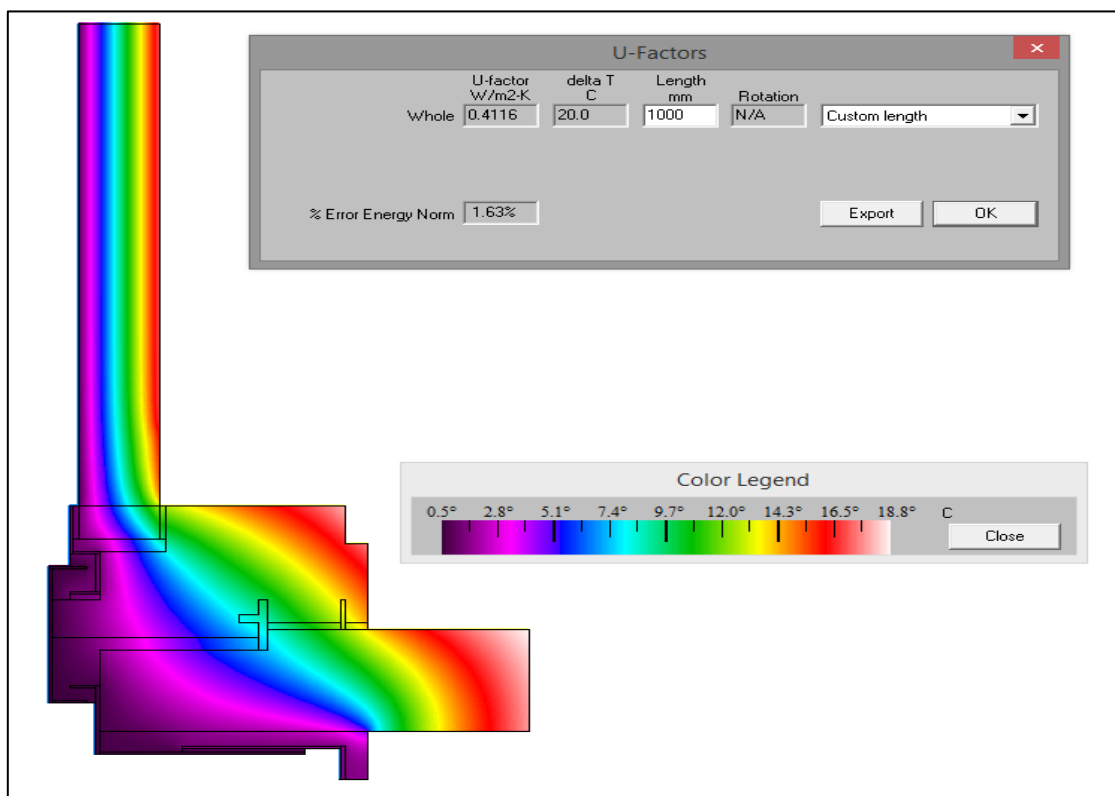


Figure 4.5.d: 2D thermal conductance and temperature distribution map of example-5

4.6 Example-6

A sliding window frame section and insulation panel is shown in Figure 4.6.a. This is the sixth example in reference [5]. A sliding window is constructed with at least two or more sections. One section is fixed and the other slides over, although it is also possible to have both sliding. Aluminium is the ideal choice for sliding profiles due to its lightweight and superior strength. It has the ability to be extruded into a wide variety of complex shapes. However, due to its high thermal conductivity, it has to be thermally broken to reduce heat losses. Polyamide (PA) and rigid polyurethane (PU) are commonly used as thermal breaks due to their low thermal conductivities. Even though both have comparable insulation features, their methods of insertion into aluminium extrusions fall into two categories. The first technique involves the insertion of a mechanical fixing and the second is to pour-and-debridge a resin material into a channel of aluminium section. The latter involves pouring special liquids chemicals, commonly polyurethane resins after temporarily connecting the indoor and exterior aluminium frame sections. Once the resin is cured, it is used as an insulating thermal barrier. The downsides of pour-and-debridge resins are that in some cases they shrink over time and hence are susceptible to leakages. Additionally, section structural strength may become weaker with time. In contrast, mechanically joined thermal breaks (e.g. polyamide inserts) maintain a good

strength and also allow different coatings/paintings to be added on either side of the finished assembly.

The model in Figure 4.6.a is constructed with multiple sections of aluminium extrusions. The indoor side and exterior side sections are separated by a polyamide break on one end, and PU strips on the other. Pile weather stripping bars are used in sliding zones, which minimise vibrations and seal out air, water and dust. The model is built with six types of materials. All unventilated air cavities of the model are shown in Figure 4.6.b. The boundary conditions assigned to the model are illustrated in Figure 4.6.c. For a 28 mm thick insulation panel separated by exterior and interior environments, thermal transmittance (U_p) is calculated as $1.13 \text{ W/m}^2\cdot\text{K}$ (see Table 3-1). The $2D$ thermal conductance (L_f^{2D}) from the FE analysis is $0.6589 \text{ W/m}\cdot\text{K}$ (see Figure 4.6.d). Parameters b_f and b_p in the FE model are 95 and 190 mm respectively. The dimension b_p is the distance between the sight-line of the insulation panel to the point of truncation of the model on the top surface. A length of 190 mm was used for simulation. The dimension b_f is the distance between bottom surface of the model and the beginning of sight-line of the insulation panel. The thermal transmittance (U_f) is $4.6757 \text{ W/m}^2\cdot\text{K}$ as per the equation (2-43).

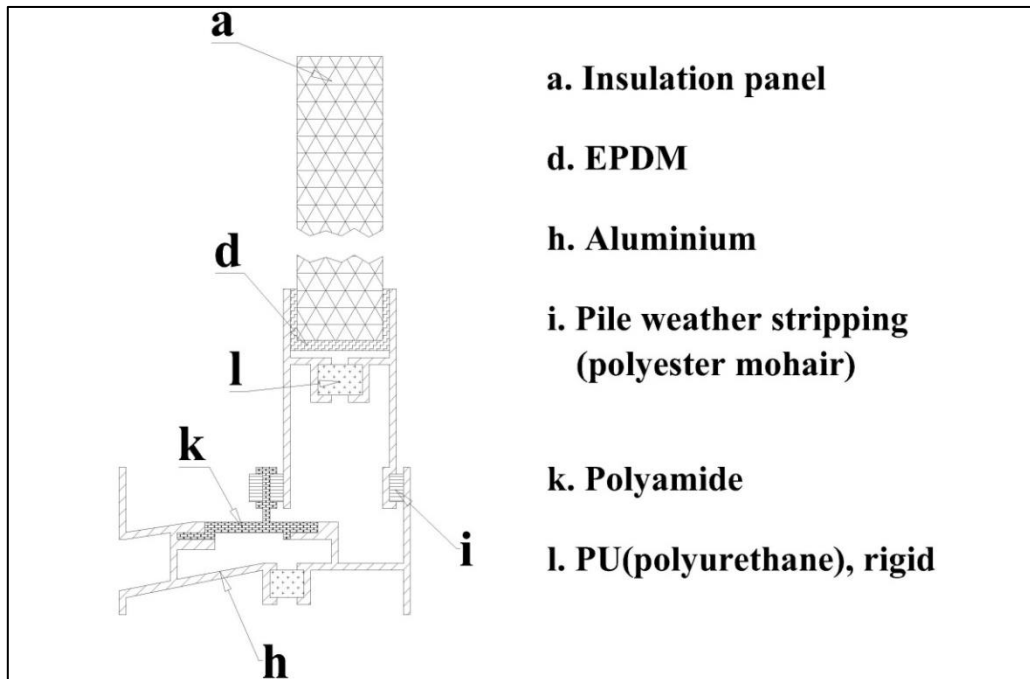


Figure 4.6.a: Illustration of example-6

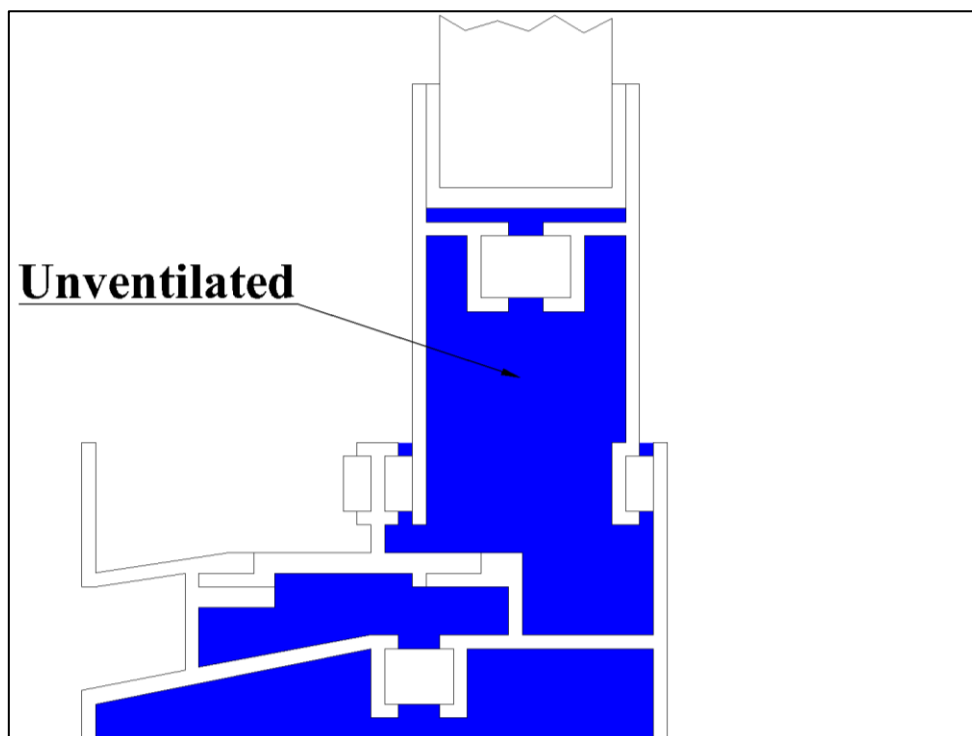


Figure 4.6.b: Unventilated air cavities of example-6

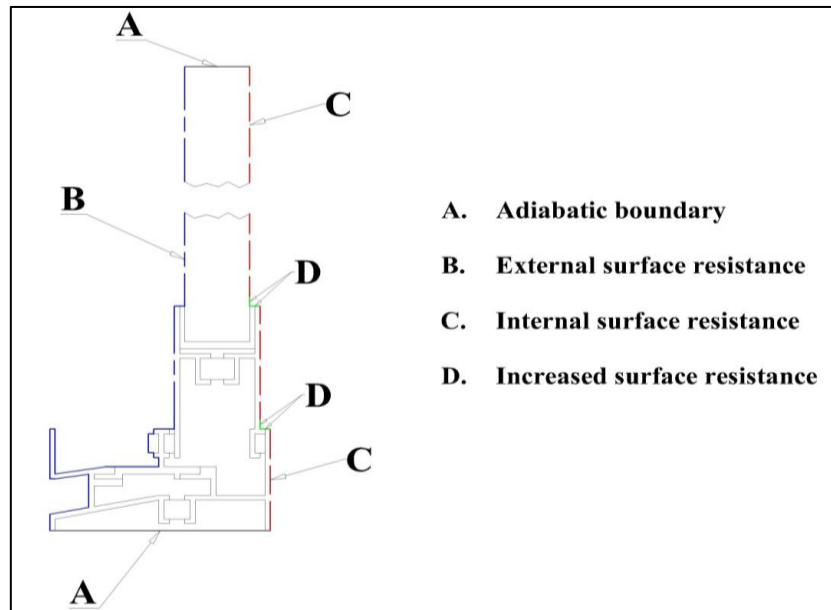


Figure 4.6.c: Illustration of boundaries of example-6

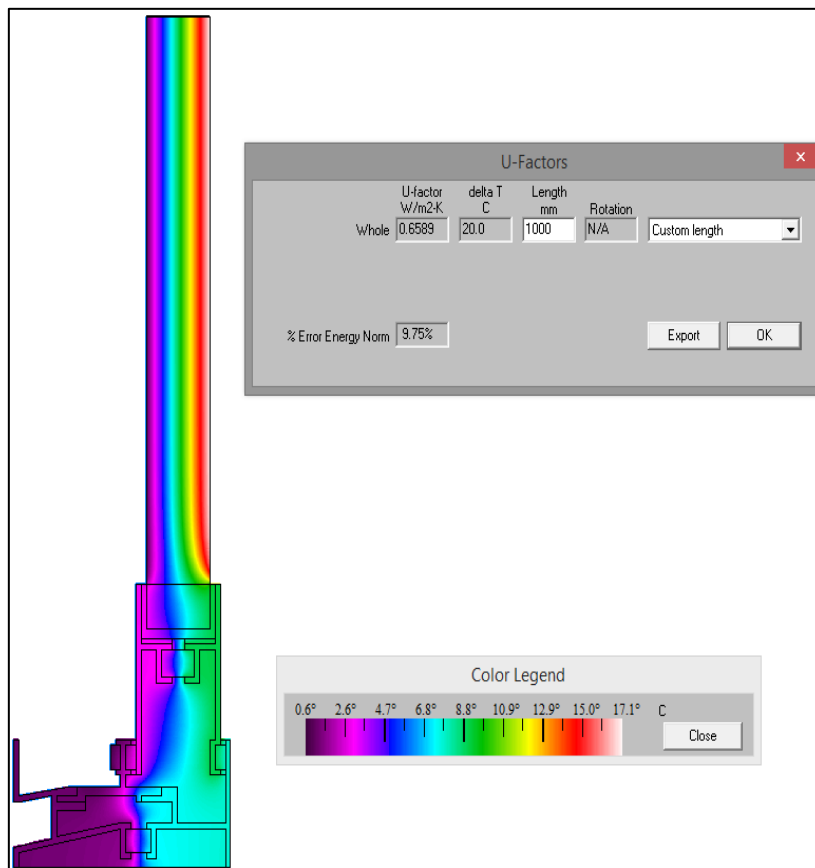


Figure 4.6.d: 2D Thermal conductance and temperature distribution map of example-6

4.7 Example-7

A fixed frame section and insulation panel is shown in Figure 4.7.a. This is the seventh example in annex-D of particular standard being used in this work [5]. This model is basically a multi-chambered frame section bonded to an insulation panel. Previously in example-3, a PVC frame constructed with steel reinforcements was simulated. Steel is used to improve the rigidity of a PVC window/door frame. Metal reinforcement makes the PVC sections far stronger but with a penalty of increased heat loss.

Multi-chambered PVC frames with no added metal reinforcements are thermally effective subject to limitations involved with structural stiffness. These designs are essentially compromises between structural stiffness and energy efficiency. The second moment of area increases with little increase in weight when frames are constructed with multiple hollow chambers. This enables them to better resist bending and buckling loads. At the same time, multi-chambered frame profiles provide unventilated air cavities that serve as natural insulators. Thus, the vast majority of PVC frames are reinforced with a stronger material to achieve a required strength.

The unventilated and slightly-ventilated type air cavities used in the model are shown in Figure 4.7.b. Four different types of boundary conditions are assigned as illustrated in Figure 4.7.c. The thermal transmittance of the insulation panel (U_p) is computed in (§3.1). For a 24 mm thick insulation panel separated by exterior and interior environments, U_p is 1.168 W/m².K (see Table 3-1). The FE simulation result of 2D thermal conductance (L_f^{2D}) is shown in Figure 4.7.d.

For a Quad Tree Mesh Parameter of 7, L_f^{2D} is 0.2854 W/m.K. The thermal transmittance of the insulation panel (U_p) is 1.168 W/m².K. The parameters b_f and b_p in the finite element model are 48 and 190 mm respectively. The dimension b_p is the distance between the sight-line of the insulation panel to the point of truncation of the model on the top surface. A length of 190 mm was used in the simulation. The dimension b_f is the distance between the bottom surface of the frame and the beginning of sight-line of the insulation panel. The thermal transmittance (U_f) is 1.3225 W/m².K as per the equation (2-43).

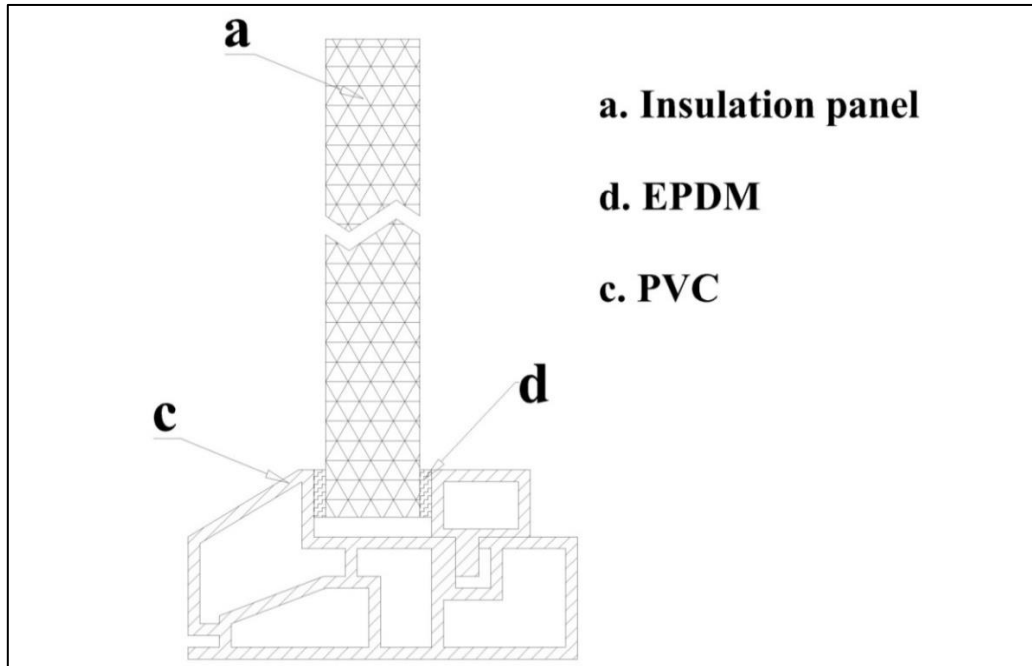


Figure 4.7.a: Illustration of example-7

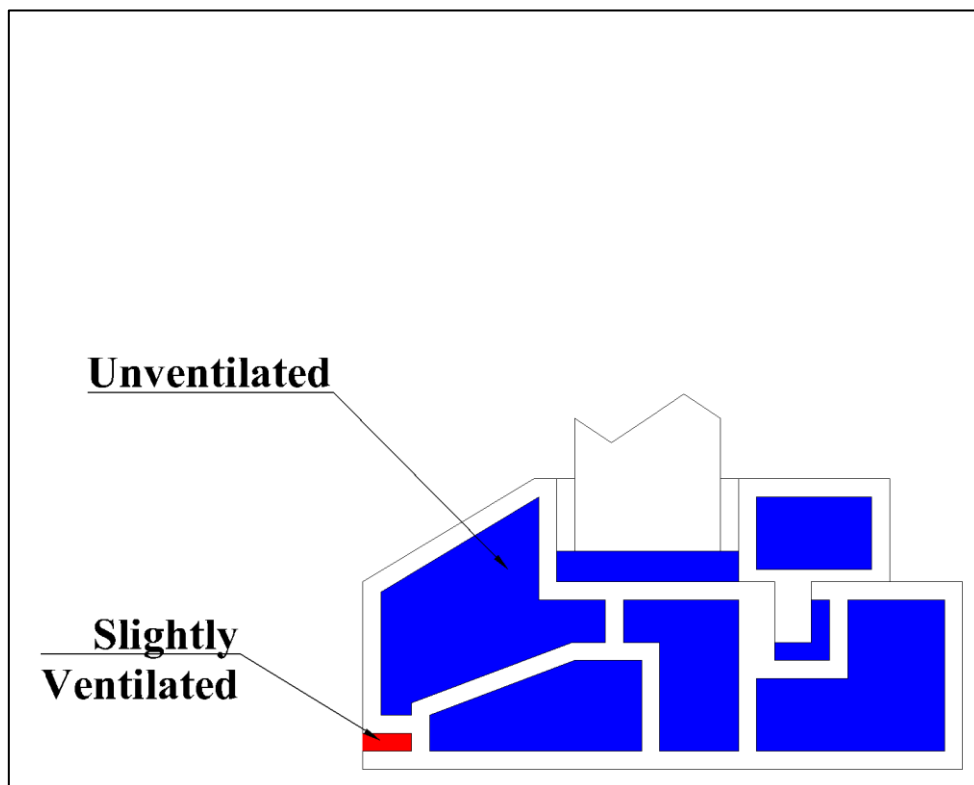


Figure 4.7.b: Air cavities of example-7.

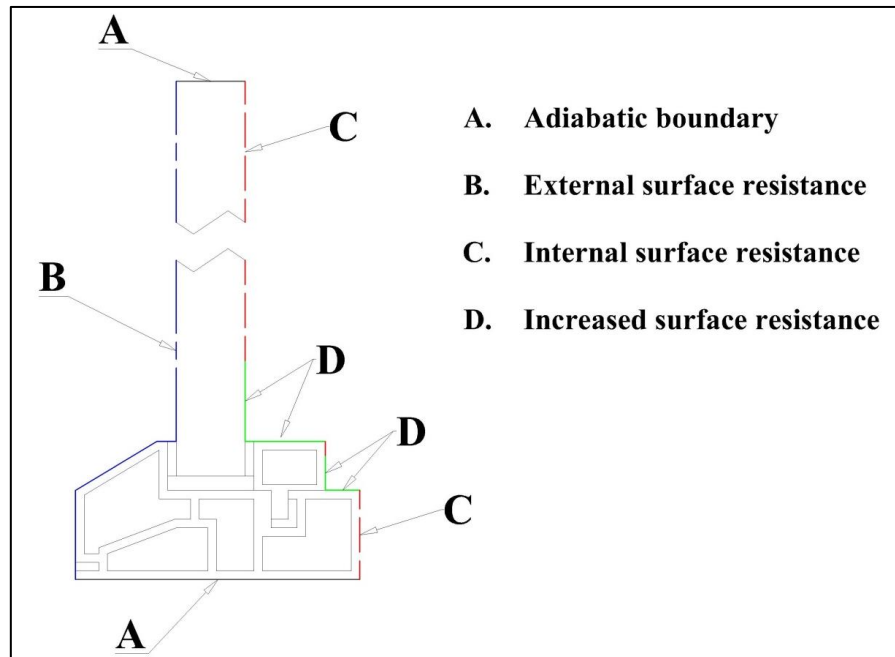


Figure 4.7.c: Illustration of boundaries of example-7.

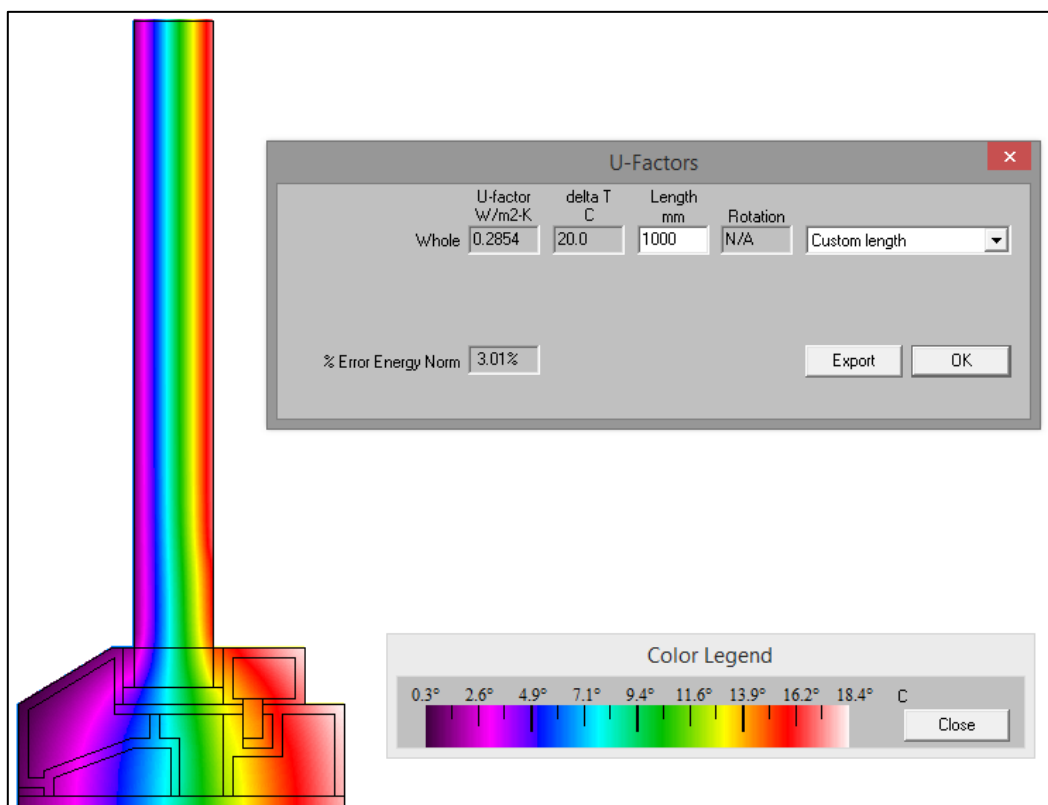


Figure 4.7.d: 2D thermal conductance and temperature distribution map of example-7

4.8 Example-8

A roller shutter box is shown in Figure 4.8.a, which is the eighth example in reference [5]. Typically, roller shutter box units are placed above a door or window, and house a chain of horizontal slats hinged together to form a slat assembly. The slats raise or lower linearly when wound or unwound leading to shutters opening or closing. The roller shutters are primary protection for windows and doors against vandalism and burglary. The PVC roller shutter box in Figure 4.8.a is of height (b_{sb}) 177 mm. Note that the slat assembly is not considered in the model. Figure 4.8.b shows the model's unventilated and slightly-ventilated type air cavities. Figure 4.8.c shows the adiabatic, interior and exterior type boundary conditions assigned to the model. The model surfaces exposed to interior and exterior environments are shown in red and blue respectively, and the adiabatic with black lines. In the simulations, the complete top surface boundary was treated as adiabatic, and left and right as external and internal respectively. The bottom surface boundary was divided into 3 zones; the left side was defined as exterior, 60 mm of its centre was treated as adiabatic and the remaining surface boundary was treated as interior as per design standard [5]. From the FE simulation, the $2D$ thermal conductance (L_f^{2D}) was obtained as 0.1844 W/m.K. A detailed temperature distribution map across the model is shown in Figure 4.8.d.

The ratio L_f^{2D} to the height of roller shutter box (b_{sb}) is taken as the thermal transmittance of the frame (U_f). The thermal transmittance (U_f) is $1.0418 \text{ W/m}^2\cdot\text{K}$ as per equation (2-45).

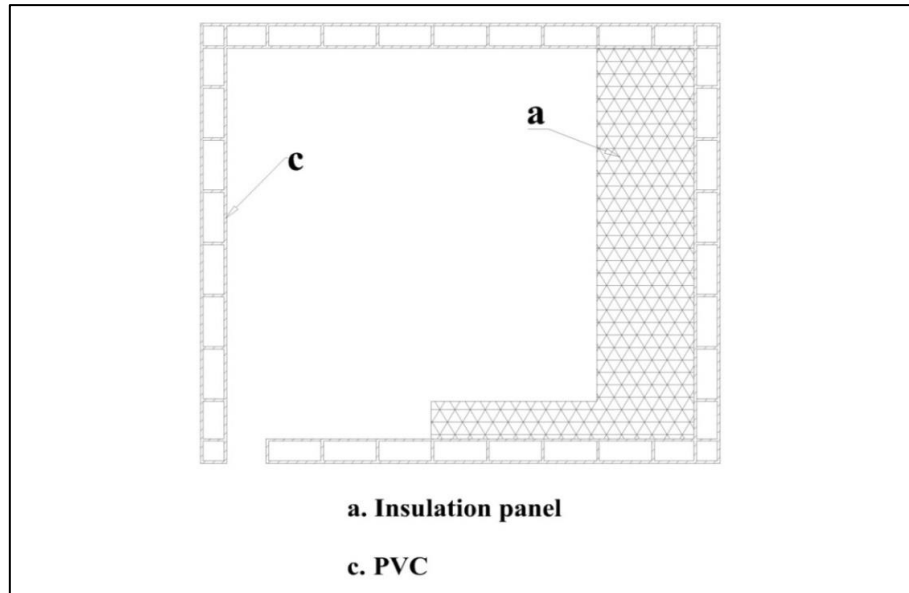


Figure 4.8.a: Illustration of example-8

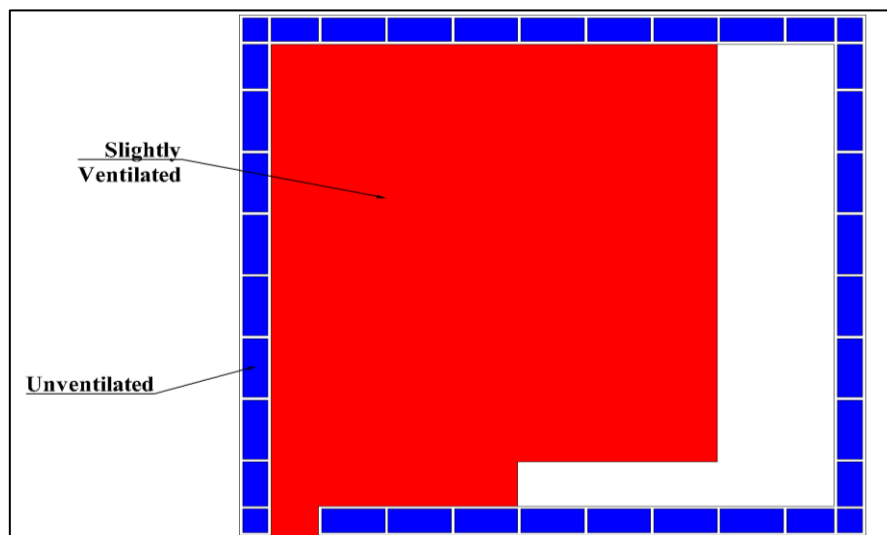


Figure 4.8.b: Air cavities of example-8.

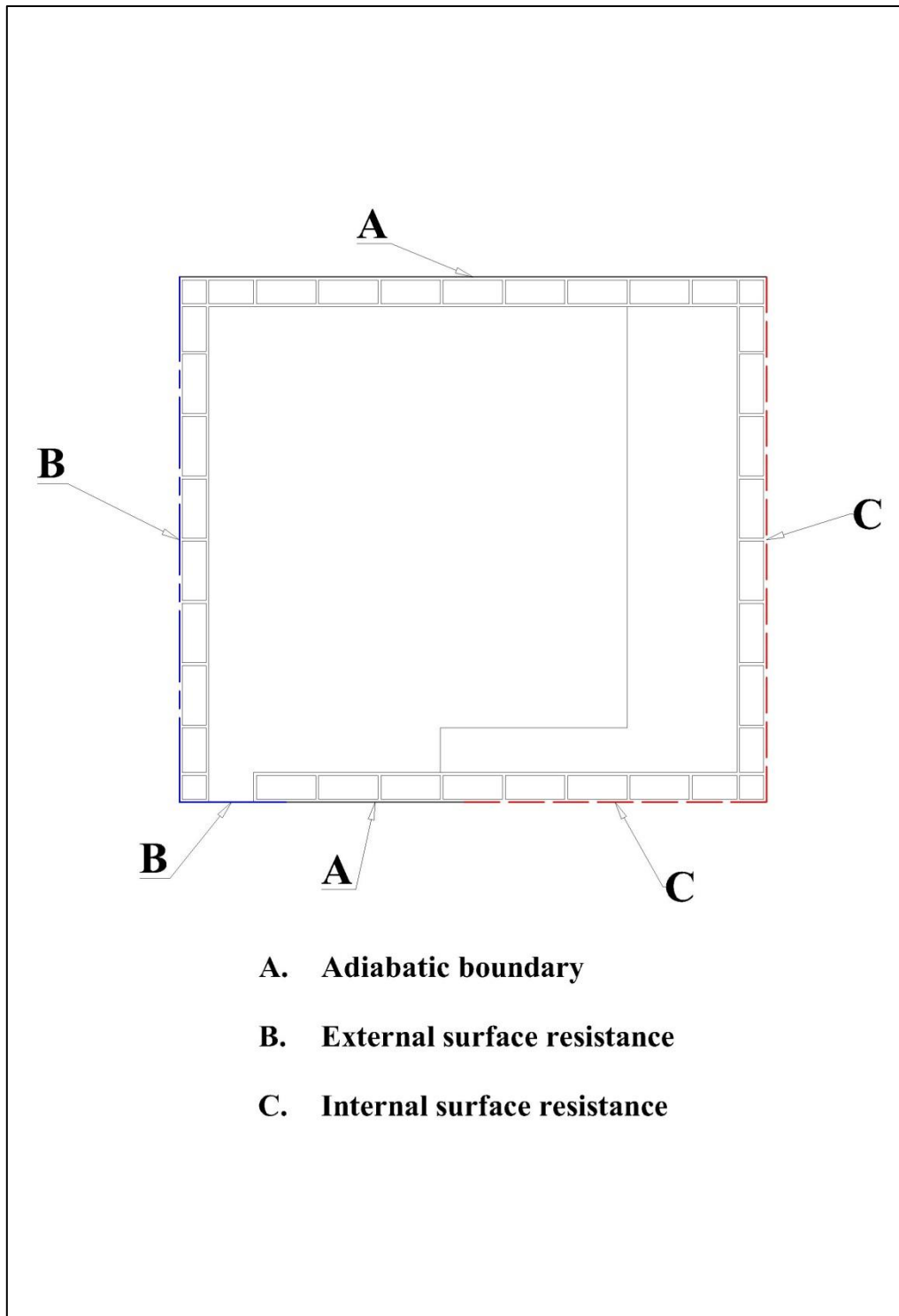


Figure 4.8.c: Illustration of boundaries of example-8

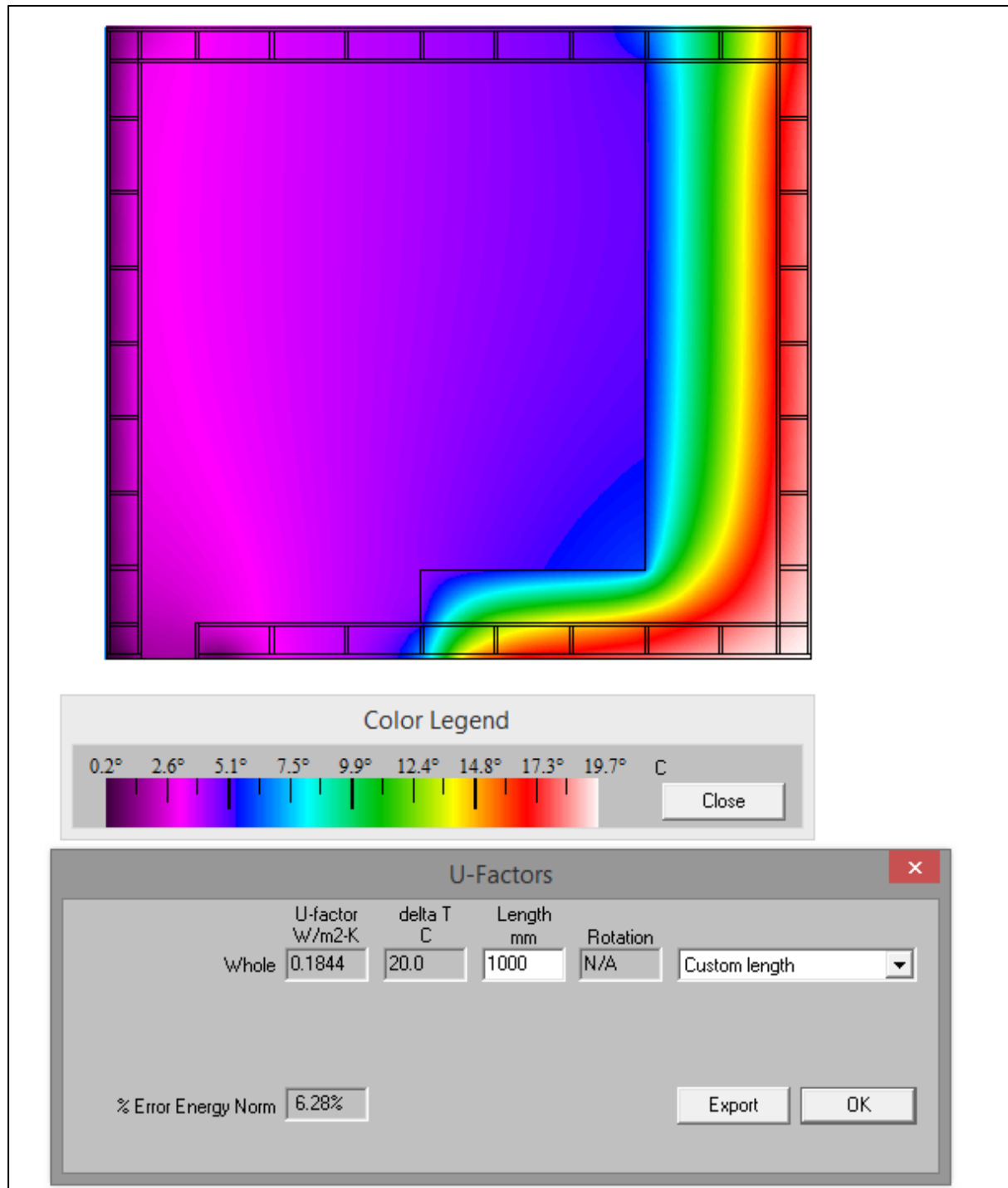


Figure 4.8.d: 2D thermal conductivity and temperature distribution map of example-8

4.9 Example-9

A PVC shutter profile of 57 mm width (b) is shown in Figure 4.9.a. This is the ninth example in annex-D from the standard [5]. The model is constructed using PVC of thermal conductivity 0.17 W/m.K. All air cavities being unventilated as shown in Figure 4.9.b. An illustration of boundary conditions assigned to the model is shown in Figure 4.9.c. The model surfaces exposed to interior and exterior environments are shown in red and blue respectively, and the adiabatic with black lines. Adiabatic, internal and exterior boundary conditions were assigned. In the FE simulations, the free surfaces to the right were treated as interior, and the left as exterior. Both the top and bottom boundaries were treated as adiabatic. The $2D$ thermal conductance (L_f^{2D}) and a detailed temperature distribution map across the model is shown in Figure 4.9.d. The ratio of L_f^{2D} to model width (b) perpendicular to the direction of heat flow is taken as the thermal transmittance of the frame (U_f).

For a Quad Tree Mesh Parameter of 7, L_f^{2D} is 0.2084 W/m.K.

The model width perpendicular to the direction of heat flow (b) is 0.057 m.

The thermal transmittance (U_f) is 3.6561 W/m².K as per equation (2-45).

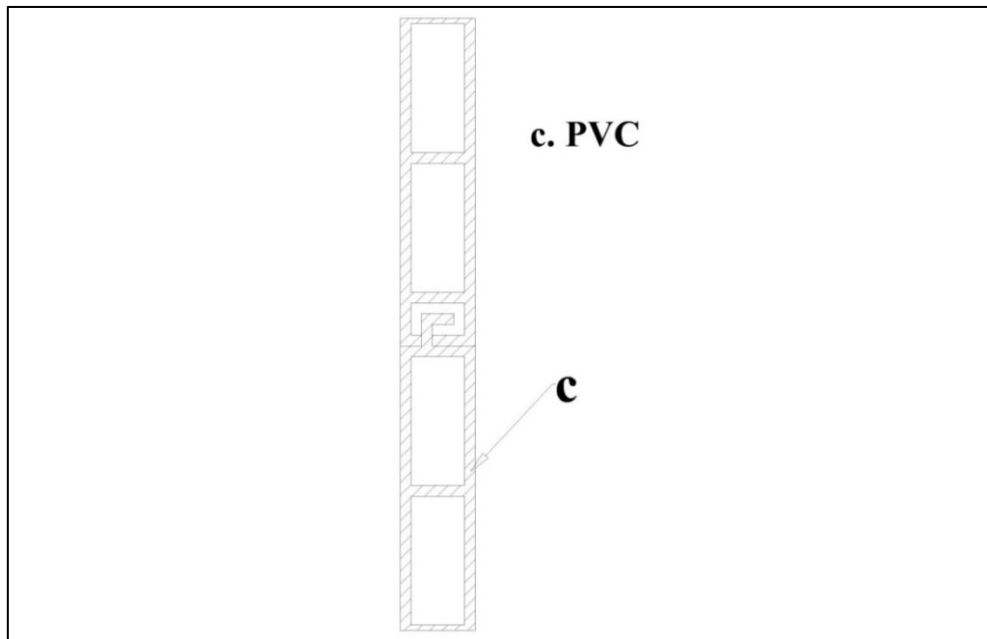


Figure 4.9.a: Illustration of example-9

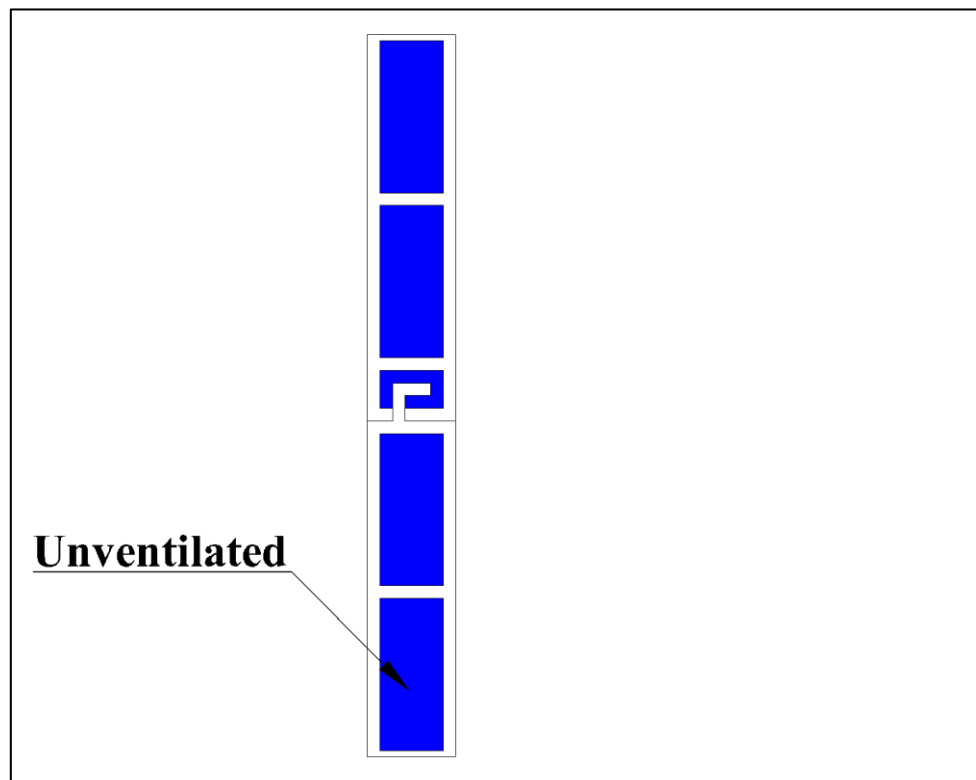


Figure 4.9.b: Unventilated air cavities of example-9

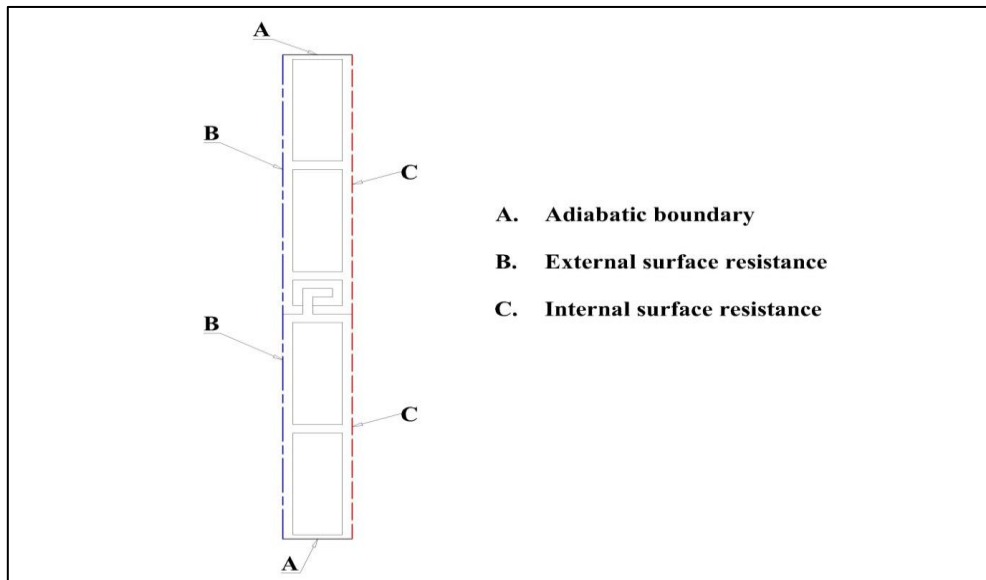


Figure 4.9.c: Illustration of boundaries of example-9

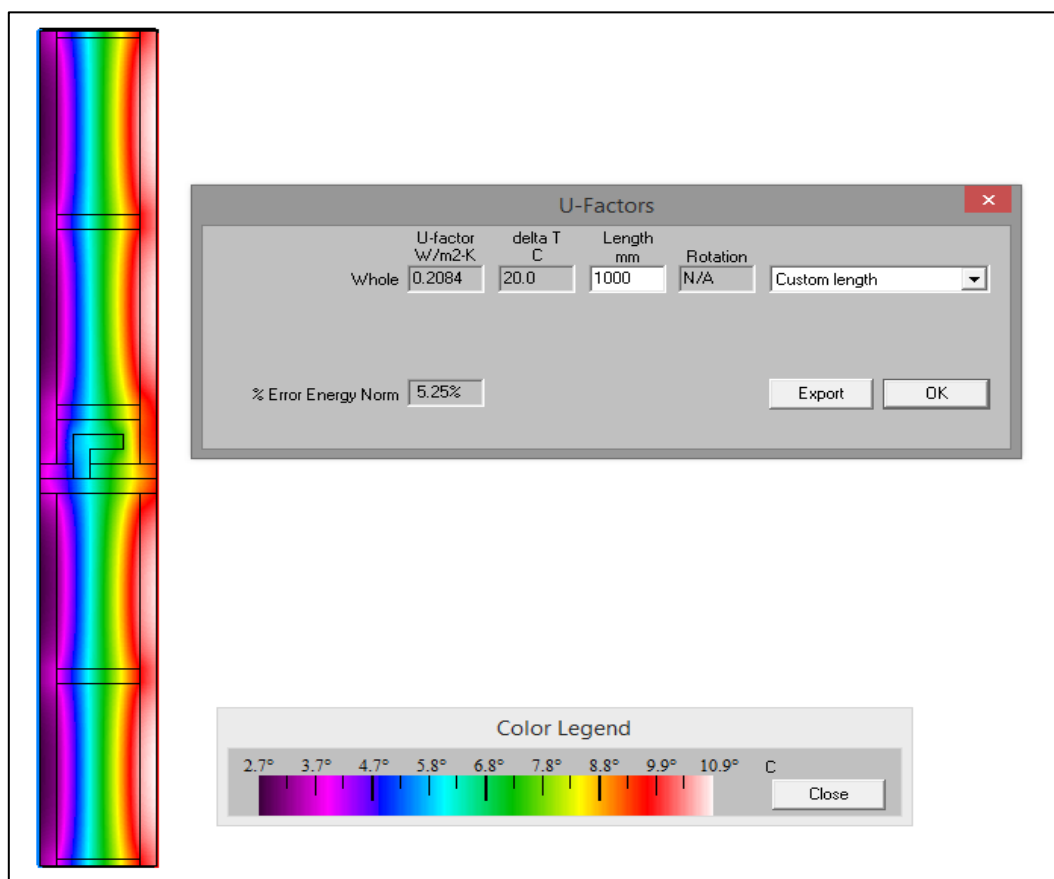


Figure 4.9.d: 2D thermal conductance and temperature distribution map of example-9

4.10 Example-10

A wood frame section with a Double Glazing Unit (DGU) is shown in Figure 4.10.a. This model is redrawn from the tenth example in reference [5]. The calculation of the linear thermal transmittance (Ψ) is a two-step process. The simulation methodology [5] states the following order:

- Simulate the frame with an insulation panel of thermal conductivity 0.035 w/m.K.
- Simulate the same frame with actual glazing and spacer configuration.

In example-4 (§4.4), the thermal transmittance of the frame (U_f) was calculated via initial simulation. The same model is extended here; a simulation is performed with the actual glazing/spacer. An illustration of the THERM finite element model is shown in Figure 4.10.a. The unventilated and slightly-ventilated type air cavities of the model are shown in Figure 4.10.b. The boundary conditions assigned are illustrated in Figure 4.10.c. The FE simulation directly provided the 2D thermal conductance of the frame-IGU assembly (L_{Ψ}^{2D}). The linear thermal transmittance (Ψ) value of the frame-IGU assembly is calculated according to equation (2-44). The centre-pane thermal transmittance (U_g) was calculated for the two-pane IGU in (§3.2).

As in example-4, the thermal transmittance of frame (U_f) was evaluated as $1.3727 \text{ W/m}^2\text{.K}$. It is used here as an input to calculate the linear thermal transmittance (Ψ) value. The centre-pane thermal transmittance (U_g) of a two-pane IGU was $1.305 \text{ W/m}^2\text{.K}$ (see Table 3-2). The 2D thermal conductance (L_{Ψ}^{2D}) and detailed temperature contours is shown in Figure 4.10.d.

For a Quad Tree Mesh Parameter of 7, L_f^{2D} is 0.4838 W/m.K .

The thermal transmittance of a two-pane glazing unit (U_g) is $1.305 \text{ W/m}^2\text{.K}$.

The thermal transmittance of the frame (U_f) is $1.3727 \text{ W/m}^2\text{.K}$.

The parameters b_f and b_g in the FE model are 110 and 190 mm respectively (Figure 2.5.b); b_g & b_f are the distances between the sight-line of the IGU to the top and bottom surfaces of the model. The linear thermal transmittance (Ψ) value is 0.08485 W/m.K as per equation (2-44).

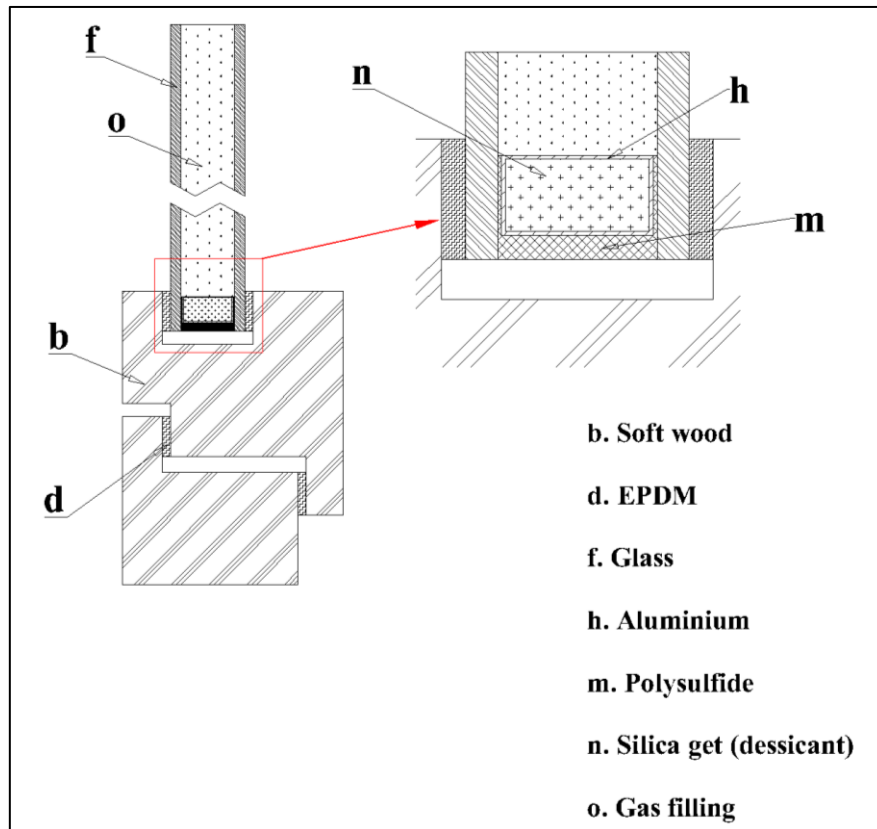


Figure 4.10.a: Illustration of example-10

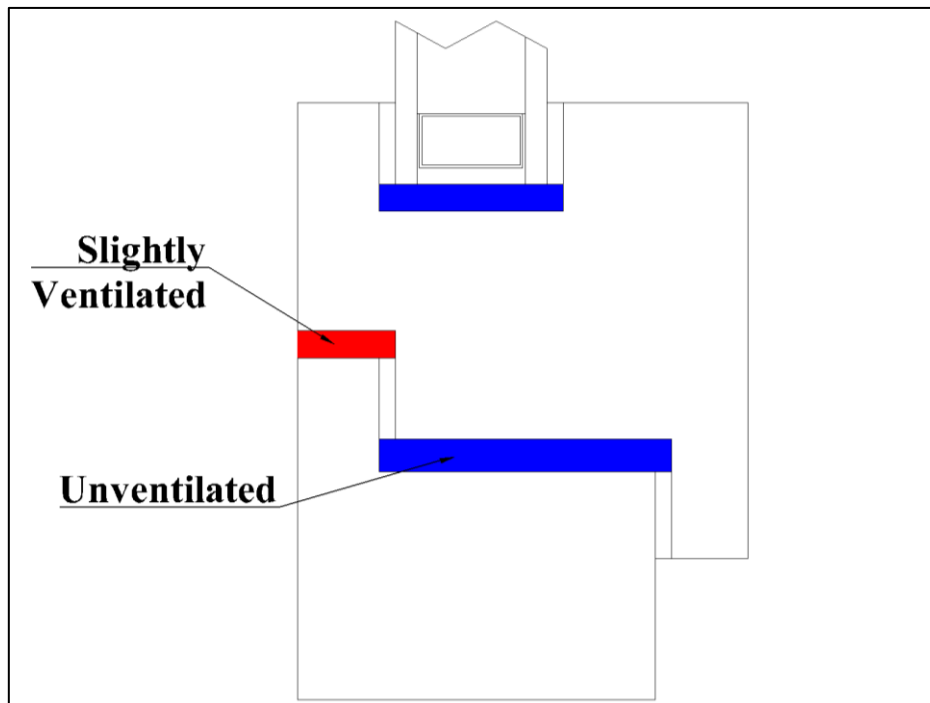


Figure 4.10.b: Air cavities of example-10

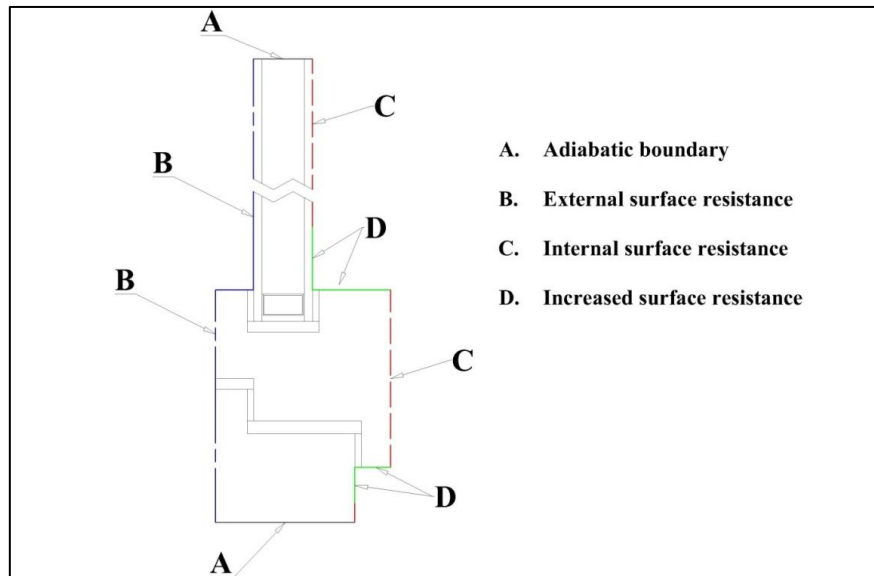


Figure 4.10.c: Illustration of boundaries of example-10

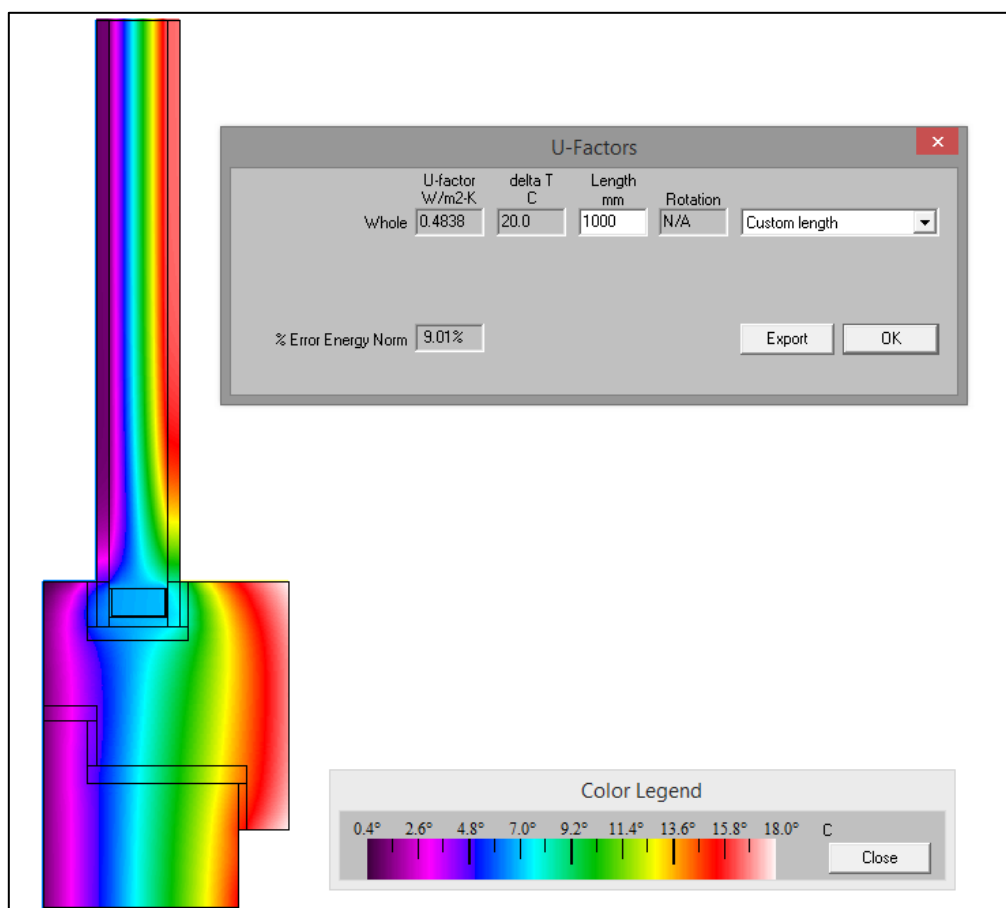


Figure 4.10.d: 2D thermal conductance and temperature distribution map of example-10

5. Conclusions

Results calculated in THERM 5.2, 6.3 and 7.1 are all identical within a 0.4% margin. The comparative studies conducted on the 10 examples indicate that the differences in results are too small to be important. This indicates that the calculation algorithms remained essentially the same between each version. The L^{2D} values for examples 1 to 9 and 10 are provided in Table 5-1 and Table 5-2 respectively. All results are within 3% of the reference values in relevant standard BS EN ISO 10077-2 [5], verifying the THERM models.

5. Conclusions

Example No	BS EN ISO 10077-2 [5]		Finite element simulation results									
			Quad Tree Mesh Parameter	THERM Version 5.2.14			THERM Version 6.3.46			THERM Version 7.1.19		
	L_f^{2D}	U_f		L_f^{2D}	U_f	% Error Energy Norm	L_f^{2D}	U_f	% Error Energy Norm	L_f^{2D}	U_f	% Error Energy Norm
1	0.550 (0.007)	3.22 (0.06)	6	0.5600	3.3118	7.04	0.5600	3.3118	7.04	0.5599	3.3109	6.97
			7	0.5599	3.3109	6.90	0.5599	3.3109	6.90	0.5598	3.3100	6.81
2	0.263 (0.001)	1.44 (0.03)	6	0.2633	1.4488	8.62	0.2633	1.4488	8.62	0.2633	1.4488	8.49
			7	0.2630	1.4460	7.35	0.2630	1.4460	7.35	0.2630	1.4460	7.49
3	0.424 (0.006)	2.07 (0.06)	6	0.4248	2.0827	7.19	0.4248	2.0827	7.19	0.4247	2.0818	7.18
			7	0.4256	2.0900	9.45	0.4256	2.0900	9.45	0.4256	2.0900	9.39
4	0.346 (0.001)	1.36 (0.01)	6	0.3470	1.3754	3.63	0.3470	1.3754	3.63	0.3469	1.3745	3.77
			7	0.3467	1.3727	2.68	0.3467	1.3727	2.68	0.3467	1.3727	2.68
5	0.408 (0.007)	2.08 (0.08)	6	0.4117	2.1323	1.84	0.4117	2.1323	1.84	0.4117	2.1323	1.84
			7	0.4116	2.1312	1.63	0.4116	2.1312	1.63	0.4116	2.1312	1.63
6	0.659 (0.008)	4.67 (0.09)	6	0.6590	4.6768	9.86	0.6590	4.6768	9.86	0.6590	4.6768	9.86
			7	0.6589	4.6757	9.75	0.6589	4.6757	9.75	0.6589	4.6757	9.75
7	0.285 (0.002)	1.31 (0.03)	6	0.2856	1.3266	4.09	0.2856	1.3266	4.09	0.2856	1.3266	4.09
			7	0.2854	1.3225	3.01	0.2854	1.3225	3.01	0.2854	1.3225	3.01
8	0.181 (0.003)	1.05 (0.02)	6	0.1849	1.0446	8.54	0.1849	1.0446	8.54	0.1850	1.0451	8.50
			7	0.1844	1.0418	6.28	0.1844	1.0418	6.28	0.1844	1.0418	6.28
9	0.207 (0.001)	3.64 (0.01)	6	0.2086	3.6596	6.88	0.2086	3.6596	6.88	0.2086	3.6596	6.88
			7	0.2084	3.6561	5.25	0.2084	3.6561	5.25	0.2084	3.6561	5.25

Table 5-1: Comparison of FE simulation and reference [5] results of examples 1 to 9

Note: The bracketed data are standard deviations from a round robin calculation reported in reference [5]

5. Conclusions

Example No	BS EN ISO 10077-2 [5]		Finite element simulation results									
			Quad Tree Mesh Parameter	THERM Version 5.2.14			THERM Version 6.3.46			THERM Version 7.1.19		
	L_{Ψ}^{2D}	Ψ		L_{Ψ}^{2D}	Ψ	% Error Energy Norm	L_{Ψ}^{2D}	Ψ	% Error Energy Norm	L_{Ψ}^{2D}	Ψ	% Error Energy Norm
10	0.481 (0.004)	0.084 (0.004)	6	0.4842	0.0849	9.79	0.4842	0.0849	9.79	0.4823	0.0842	5.90
			7	0.4838	0.0848	9.01	0.4838	0.0848	9.01	0.4838	0.0848	9.42

Table 5-2: Comparison of FE simulation and reference [5] results of example 10

Note: The bracketed data are standard deviations from a round robin calculation reported in reference [5]

References

- [1] Approved Document L1A: Conservation of Fuel and Power (New Dwellings) - by Communities and Local Government, RIBA Publications, 2010. ISBN-13: 9781859463246.
- [2] Programmes to Reduce Household Energy Consumption — House of Commons papers 1164 2007-08, Great Britain National Audit Office, TSO Publications. ISBN: 9780102954357.
- [3] Xavier García Casals, Analysis of building energy regulation and certification in Europe: Their role, limitations and differences, Energy and Buildings, Volume 38, Issue 5, May 2006, Pages 381-392, ISSN 0378-7788.
- [4] Waters, J.R. Energy conservation in buildings: a guide to part L of the building regulation. Blackwell Publishing Ltd, 2003. Oxford OX4 2DQ. ISBN 9781405112536.
- [5] BSI Standards. Thermal performance of windows, doors and shutters — Calculation of thermal transmittance — Part 2: Numerical methods for frames. BS EN ISO 10077-2: 2012, ISBN 978 0 580 68943 7.
- [6] THERM. Windows and Daylighting Group, Building Technologies Department, Environmental Energy Technologies Division, Ernest Orlando Lawrence Berkeley National Laboratory, Berkeley CA 94720, USA.
- [7] Hutton, D.V. Fundamentals of finite element analysis (Book), 1st edition 2004, McGraw-Hill companies, Inc. ISBN 0-07-112231-1.

- [8] Nguyen, D.T. Finite Element Methods: Parallel-Sparse Statics and Eigen-Solutions (Book). ISBN 978-0-387-29330-1, 2006 Springer science Inc.
- [9] Bathe, K.-J. Finite Element Procedures (Book). ISBN 0-13-301458-4, 1996 by Prentice-Hall, Inc.
- [10] ANSYS Inc. Southpointe, 275 technology Drive, Canonsburg, PA 15317.
- [11] ABAQUS Unified FEA. Dassault Systèmes, Rising Sun Mills, 166 Valley Street, Providence, RI 02909-2499, USA.
- [12] ADINA R & D, Inc. 71 Elton Avenue, Watertown, MA 02472, USA.
- [13] Altair Engineering, Inc. 1820 East Big Beaver Rd, Troy, MI 48083.
- [14] Dhondt, G. “CALCULIX” finite element code. Available [online] at: <http://www.dhondt.de>
- [15] Flixo pro. Informind Ltd, Weberstrasse 10, CH-8004 Zurich, Switzerland.
- [16] Frame Simulator. DaeTWin. VIA S.CATERINA, 17, 36061 Bassano del Grappa (VI), Italy.
- [17] Rao, S. S. The Finite Element Method in Engineering (Book). Butterworth-Heinemann Ltd, 2004. ISBN 10: 0-7506-7828-3.
- [18] Cook, R.D. Finite element modeling for stress analysis (Book). John Wiley & Sons, 1995. ISBN: 0-471-10774-3.
- [19] Zienkiewicz, O.C and Zhu, J.Z. The superconvergent patch recovery and a posteriori error estimates. Part 1: The recovery technique.

- International journal for numerical methods in engineering. Vol 33, pp.1331-1364,1992.
- [20] Zienkiewicz, O.C and Zhu, J.Z. The superconvergent patch recovery and a posteriori error estimates. Part 2: The error estimates and adaptivity. International journal for numerical methods in engineering. Vol 33, pp. 1365-1382,1992.
- [21] Lawrence Berkeley National Laboratory. 1 Cyclotron Rd, Berkeley, California 94720, USA.
- [22] WINISO. Sommer Informatik GmbH, Sepp-Heindl-Str. 5, 83026 Rosenheim, Germany.
- [23] BISCO. Physibel, Heirweg 21, B-9990 Maldegem, Belgium.
- [24] HEAT2. BLOCON USA, 27 Hillcrest Rd, Reading, MA 01867, USA.
- [25] Autodesk, Inc. 111 McInnis Parkway, San Rafael, CA 94903, USA
- [26] Dassault Systemes SolidWorks Corporation. 175 Wyman Street, Waltham, MA 02451,USA.
- [27] IMSI/Design,LLC. 25 Leveroni Ct, Novato, CA 94949, USA.
- [28] PTC Creo, 140 Kendrick street, Needham, MA 02494, USA.
- [29] Mitchell, R., Kohler, C., Curcija, D., Zhu, L., Vidanovic, S., Czarnecki, S and Arasteh, Dariush., Carmody, J and Huizenga, C. THERM 6.3/WINDOW 6.3 NFRC Simulation Manual.
- [30] Arasteh, D., Finlayson, E., Rubin, M and Sadlier, J. Recent technical improvements to the WINDOW computer program. Lawrence

- Livermore National Laboratory Report-41680, 1995. Available [online] at:
<http://eetd.lbl.gov/sites/all/files/publications/41680.pdf> [Accessed on 25th June 2014]
- [31] Shapiro, A.B. TOPAZ2D: a two-dimensional finite element code for heat transfer analysis, electrostatic, and magnetostatic problems. Lawrence Livermore National Laboratory. Report UCID-20824, 1986.
- [32] Shapiro, A.B. FACET – a radiation view factor computer code for axisymmetric, 2D planar, and 3D geometries with shadowing. Lawrence Livermore National Laboratory. Report UCID-19887, 1983. Available [online] at:
<http://www.osti.gov/scitech/servlets/purl/5607653> [Accessed on 25th June 2014]
- [33] Mitchell, R., Kohler, C., Arasteh, D., Carmody, J., Huizenga, C and Curcija, D. THERM 5.2/WINDOW 5.2 NFRC Simulation Manual. LBNL-48255. Available [online] at:
<http://windows.lbl.gov/software/NFRC/NFRCSim5.2-July06Version.pdf> [Accessed on 25th June 2014]
- [34] Motte, A. Newton's Principia mathematica –The Mathematical Principles of Natural Philosophy by Sir Isaac Newton. First Edition, Published by Daniel Adee, 45 Liberty Street, New York. Available [online] at:

https://openlibrary.org/books/OL7089085M/Newton%27s_Principia
[Accessed on 5th July 2014]

- [35] Fourier, J. The analytical theory of heat (Book). Cambridge University Press 2009. ISBN 978-1-108-00178-6.
- [36] Holman, J.P. Heat transfer (Book). McGraw-Hill, 1989. ISBN: 0-07-100487-4.
- [37] Rogers, G.F.C and Mayhew, Y.R. Engineering thermodynamics work and heat transfer (Book). PEARSON Prentice Hall, 4th Edition, 1992. ISBN-978-0-582-04566-8.
- [38] Donald, R.P and Leighton, E.S. Theory and problems of heat transfer (Book). Schaum's outline series, second edition 1997, McGraw-Hill. ISBN 0-07-050207-2.
- [39] Howell, J.R. Thermal Radiation Heat Transfer, 5th Edition, Taylor & Francis Publishers 2002. ISBN 1-56032-839-8.
- [40] BSI Standards. Glass in building - Determination of thermal transmittance (U value) — Calculation method. BS EN 673:2011, ISBN 978 0 580 71226 5.
- [41] Nammi, S.K., Shirvani, H., Shirvani, A., Edwards, G and Dunn, J. Spreadsheet tools to estimate the thermal transmittance and thermal conductivities of gas spaces of an Insulated Glazing Unit. ISBN: 978-0-9565608-7-2. Available [online] at:
<http://hdl.handle.net/10540/313715> [Accessed on 23rd June 2014]